minerals

Article

The Middle Miocene Microfacies, Cyclicity, and Depositional History: Implications on the Marmarica Formation at the Siwa Oasis, Western Desert (Egypt)

Mohamed A. Khalifa [1], Amr S. Zaky [1,2,*], Luigi Jovane [2,*], Ahmed M. El-Hewy [3], Esam Zahran [3] and Atef M. Kasem [3]

[1] Geology Department, Faculty of Science, Menoufia University, Shebin El-Kom 32511, Egypt; khcycle1949@gmail.com
[2] Instituto Oceanográfico, Universidade de São Paulo, Praça do Oceanográfico, 191, São Paulo 05508-120, Brazil
[3] Geology Department, Faculty of Science, Damanhour University, Damanhour 22511, Egypt; ahmedelhewy93@gmail.com (A.M.E.-H.); esam.zahran@yahoo.com (E.Z.); kasematef@sci.dmu.edu.eg (A.M.K.)
* Correspondence: amrsaid86@science.menofia.edu.eg or amr.zaky@usp.br (A.S.Z.); jovane@usp.br (L.J.)

Abstract: Microfacies studies were carried out on the Middle Miocene Marmarica Formation exposed at the Gabal Western Bahi El-Din and Gabal El-Najdeen, the Siwa Oasis, northwestern Desert (Egypt). It was distinguished into the lower, middle, and upper members. Eleven microfacies types were recognized, which include skeletal lime-mudstone, dolomitic lime-mudstone, intraclastic wackestone, bryozoan wackestone, foraminiferal wackestone, foraminiferal bryozoan packstone, glauconitic molluscan packstone, molluscan intraclastic packstone, pelletal peloidal skeletal packstone, dolostones, and claystone microfacies. This formation includes several types of emergence- meter-scale cycles (shallowing-upward). Field observations and petrographic analyses revealed that these cycles consist of pure carbonates and mixed siliciclastic carbonates. These cycles consist of four types of gradual cycles and six types of non-gradual cycles. The gradual emergence cycles indicate a balance between the rate of subsidence, sea level oscillations, and sedimentation rate. The non-gradual cycles indicate an irregular balance between sedimentation rate and subsidence rate. The non-gradual cycles denote high-frequency sea level variation and/or short-term sea level oscillations, which are associated with high carbonate formation. The depositional environments of the Marmarica Formation are restricted to lagoonal at the base, followed upward to open marine conditions. Both environments most probably characterize the platform setting.

Keywords: Siwa Oasis; Miocene; Marmarica Formation; microfacies; depositional environment; cyclicity

check for updates

Citation: Khalifa, M.A.; Zaky, A.S.; Jovane, L.; El-Hewy, A.M.; Zahran, E.; Kasem, A.M. The Middle Miocene Microfacies, Cyclicity, and Depositional History: Implications on the Marmarica Formation at the Siwa Oasis, Western Desert (Egypt). *Minerals* **2024**, *14*, 73. https://doi.org/10.3390/min14010073

Academic Editor: János Haas

Received: 11 November 2023
Revised: 14 December 2023
Accepted: 28 December 2023
Published: 8 January 2024

1. Introduction

The Middle Miocene (ca. 16–11.6 Ma) is one of the most interesting time intervals in Earth history regarding global climate change [1]. It witnessed two climatic and environmental shifts; the first is known as the Middle Miocene Climatic Optimum (MMCO), and the second (about 15–13 Ma) is called the Middle Miocene Climatic Transition (MMCT). During the MMCO, warm conditions prevailed and perhaps lasted as long as the present day during the whole period of the Middle Miocene [1,2]. A transition to global cooling, the expansion of Antarctic ice sheets [3–5], and eustatic sea level fall [6–8] were noted during the MMCT. The Miocene carbonates cover most of the Mediterranean regions [9–11]. Remarkably homogeneous shallow-marine carbonates were deposited along the southeast Mediterranean Sea coast throughout much of the northern western Desert of Egypt [12] and the Cyrenaica region of north-eastern Libya [13]. In the northern western Desert, the Miocene carbonates are outcropping between Sidi Barani and Salum along a northern escarpment that faces the Mediterranean Sea and between the Qattara Depression and Siwa Oasis along a southern escarpment (Figure 1).

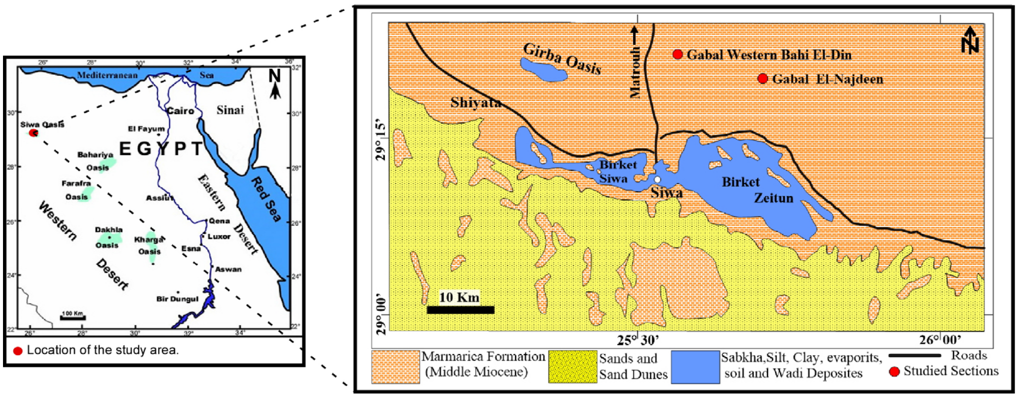

Figure 1. A location and simplified geological map of the Siwa Oasis, Western Desert (Egypt).

The northwest side of the Siwa Oasis is surrounded by exposed sedimentary successions belonging to the Marmarica Formation. Several studies were carried out on this formation in terms of microfacies analysis, petrography, and stratigraphy [14–19]. The most important previous lithostratigraphic studies on the study area in comparison to the present study are represented by Table 1. The Marmarica Formation consists of thick, mostly horizontal carbonate rocks and covers almost the whole northern extent of the Western Desert [20–22]. It was assigned to the Middle Miocene [12,14,20]. At the El-Diffa plateau (north Siwa Oasis), it overlies the Mamoura Formation and the Lower Miocene Moghra Formation in most other areas [21]. It has a wide geographic distribution, extending from the Nile Delta in the east to Salum City in the west. Moreover, it extends westwards beyond the Salum and enters Libya parallel to the Mediterranean Sea until Toprock City (eastern Libya).

Table 1. Lithostratigraphic classifications of the Miocene rocks by different authors in the northwestern Desert (Egypt).

Series/ Epoch		Stage/ Age	Rock Units	[20]	[14] Siwa Oasis	[23] North-Western Desert (Subsurface)	[24]	[25] Northeastern Libya	[19]	[16]	[17]	Present Study	
Miocene	Middle	Serravallian	Marmarica Fm.	Marmarica Fm.	El-Diffa Plateau mb.	Marmarica Fm.	Marmarica Fm./ Gairabub Fm.	Al-gaghboub Fm.	Marmarica Fm.	El-Diffa Plateau mb.	El-Diffa Plateau mb.	Marmarica Fm.	upper mb.
					Siwa Escarpment mb.					Siwa Escarpment mb.	Siwa Escarpment mb.		middle mb.
		Langhian			Oasis mb.					Oasis mb.	Oasis mb.		lower mb.
	Early	Burdigalian	Moghra Fm.	Moghra Fm.	Moghra Fm.	Not-studied			Moghra Fm./ Mamoura Fm.	Moghra Fm.	Moghra Fm.	Moghra Fm.	
		Aquitanain											

This formation outcrops at the cliffs that extend along the Mediterranean coast and is composed mainly of alternating limestone, dolostone, and claystone [21]. At the western outcrops, its thickness varies from 78 to 104 m at Minqar Tabagh, at the extreme western tip of the Qattara Depression [22]. It gradually decreases in thickness eastward and changes to a mainly clastic sequence with few limestone beds. Further eastwards, it changes entirely to evaporites, about 6 m thick [22]. Moreover, this formation was subdivided at the Siwa Oasis [14,17].

Shedding light on the Marmarica Formation at the Siwa Oasis, Western Desert (Egypt), will contribute to a better understanding of the sea level oscillations and paleoenvironmental conditions that prevailed during the Middle Miocene and resulted in carbonate deposition along the marine shelf encircling western and northern Africa [17]. The main objectives of this study are to provide a detailed lithostratigraphic description of this study sections, identify the different microfacies, determine their depositional environments, and track the cyclicity of this study interval.

2. Materials and Methods

The Marmarica Formation was investigated in two different sections located at the Siwa Oasis. The first section is exposed at Gabal Western Bahi El-Din, which is located at Latitude 29°26′020″ N and Longitude 25°33′561″ E. The second section occurs at Gabal El-Najdeen at Latitude 29°23′068″ N and Longitude 25°426′04″ E (Figure 1). A total of 435 fresh rock samples were collected from this study sections and wherever lithologic changes were noted. The field work included the collection of lithologic samples and macrofossils, the description of the primary structures, and identifying the different depositional cycles as well as their depositional environments. Laboratory studies include the examination of sixty-seven (67) thin sections representing the beds of the Marmarica Formation by using a Euromex polarizing light microscope at the Department of Geology, Damanhour University (Egypt). The classification of [26], modified by [27], was adopted for remarking the different microfacies types of limestones. Furthermore, ten (10) shale samples from the two studied sections were examined by X-ray diffraction (XRD), and eight (8) dolomitic limestone samples were examined and scanned at the Faculty of Science, Alexandria University (Egypt) by the JSM-IT 200 (JEOL) scanning electron microscope (SEM).

3. Geological Setting

The Siwa Oasis is located on the northwestern side of the Western Desert of Egypt, near the southern edge of the El-Diffa Plateau (Figure 1) and within the tectonically unstable African cratonic border [12] as a part of the North African passive continental margin. The northern Western Desert was subjected to different structural tectonic phases, especially during the Oligo-Miocene [28]. The "Alpine Orogeny" was the result of the convergence of the European and African plates. As a result, the Tethys was closed from the late Cretaceous to the present, the Atlas Mountains have risen, and a general pulsed compressional regime has developed throughout North Africa. Moreover, there was rapid regression of the Tethys after the late Eocene, and concurrent uplift and deposition of the clastic deposits were formed and named the Qatrani Formation [29]. The Qatrani Formation changes northwestward to give rise to the deposition of the inner marine marl of the Dabaa Formation. During the Oligo-Miocene, there was a last rift that affected the North African region and resulted in the evolution of the Red Sea Rift, the East African Rift System, and the Gulf of Aden [30]. This phase is called the Alpine movement, which culminated from the beginning of the Oligocene to the end of the Miocene. From the Late Miocene to the Late Quaternary, there was NW-SE faulting and intense volcanic activity associated with rifting in eastern North and central Africa [29]. Volcanic activity in this phase resulted in the formation of the basaltic plateau (northern Libya), the Qatrani volcanics (Egypt), the Tibesti volcanoes (southeast Libya), the Jebel Haruj's volcanics (Central Libya, northern east Chad), and Hoggar's volcanism (northeast Mali, northwest Niger, and south Algeria).

4. Lithostratigraphy

The Middle Miocene Marmarica Formation was introduced by [20] to describe the vast portion of the northern carbonate plateau of the Egyptian Western Desert. Its type locality occurs near Siwa town (about 5 km to the north) at the northern escarpment of Siwa Oasis [20]. It has a thickness of around 78 m of a biogenic carbonate with intercalations of marls and shales [20]. The base of the Marmarica Formation is unexposed [12]. It unconformably overlies the Moghra Formation or the Raml Formation [12] and unconformably underlies the Pliocene–Pleistocene rocks in the Wadi El-Natrun. On the other hand, it conformably overlies the Moghra Formation (Lower Miocene) in the walls of the Depression of Qattara [22]. They added that southwards at the Qattara-Wadi El Natrun stretch, it unconformably overlies the Lower Miocene Raml Formation. Its upper boundary unconformably underlies the Early Pleistocene Gar El Muluk Formation. Further northwards, it is uncovered between the coast of the Mediterranean and the Qattara, except for some loose sand and gravel, or by Pliocene-Pleistocene limestone crust [22]. Eastwards, the Marmarica Formation exhibits lateral facies changes to evaporites that are assumed to be about 10 m thick. However, it grades to marls and becomes a sandy limestone unit near Alamein, and the faunal unit is remarkably uniform [12]. Westwards, it is entirely composed of limestone, with increasing thickness reaching up to 160 m adjacent to the Salum area [22]. Further westwards, beyond the Salum, the Marmarica Formation has the same lithological components (mainly carbonate facies) and enters the Libyan Desert with a new term called the Gaghbub Formation.

Moreover, the Marmarica Formation has been classified into two informal members from base to top: the lower member, which consists of gray calcarenites with intercalations of shale, and the upper member, which consists of pure white limestone [20]. Furthermore, [14] subdivided the Miocene sequence outcropped at the Siwa area into three formal members (the Oasis Member, the Siwa Escarpment Member, and the El-Diffa Plateau Member). They documented that the Oasis Member (Early Middle Miocene) belongs to the Moghra Formation, which is composed of marine facies and cross-bedded coquina and coquina-marl shale intercalated with other mechanical carbonate rocks. The Siwa Escarpment Member (Middle Miocene) belongs to the lower member of the Marmarica Formation and consists of white chalky limestone. The El-Diffa Plateau Member (Middle Miocene) belongs to the upper member of the Marmarica Formation, and it consists of highly fossiliferous chalky limestone alternating with poorly fossiliferous chalky marl or chalk. Later, several authors followed [14] in their subdivision of the Marmarica Formation, such as [16,17,31–34].

5. Results

5.1. Lithostratigraphy

The present study followed the subdivision of [14] for the Marmarica Formation at the Siwa Oasis. Indeed, it can be classified into lower, middle, and upper members. A detailed description of these members based on field studies and observations is documented below:

5.1.1. The Lower Member

This member is about 22 m and 18.5 m thick at the Gabal Western Bahi El-Din and Gabal EL-Najdeen sections, respectively (Figures 2 and 3A,B). It unconformably overlies the Moghra Formation (Figure 3C). It consists of fossiliferous limestones interbedded with sandy limestones, dolomitic limestone, calcarenite limestone, argillaceous marley fossiliferous limestone, and thin beds of shale. The limestone beds of this member are reddish yellow, brownish, yellowish white, yellow, and white, fossiliferous, argillaceous, gypseous, massive, and sandy. The shale beds are green and greenish yellow, thin-bedded, glauconitic, highly calcareous, jointed, and fractured, fossiliferous, fissile, thin-laminated, and contain gypsum bands and veins (Figure 3D). The macrofossils recorded in this member include *Pecten* sp. and *Oyster* sp. of pelecypods and *Turritella* sp. of gastropods (Figure 3E). The top part of this member is characterized by the presence of several horizontal and vertical burrows of *Thalassinoides* (Figure 3F) and the occurrence of syndeposition structures (Figure 3A). The top part of this member is characterized by the occurrence of a pecten bed, which attains a thickness of about 0.6 m (Figure 4A).

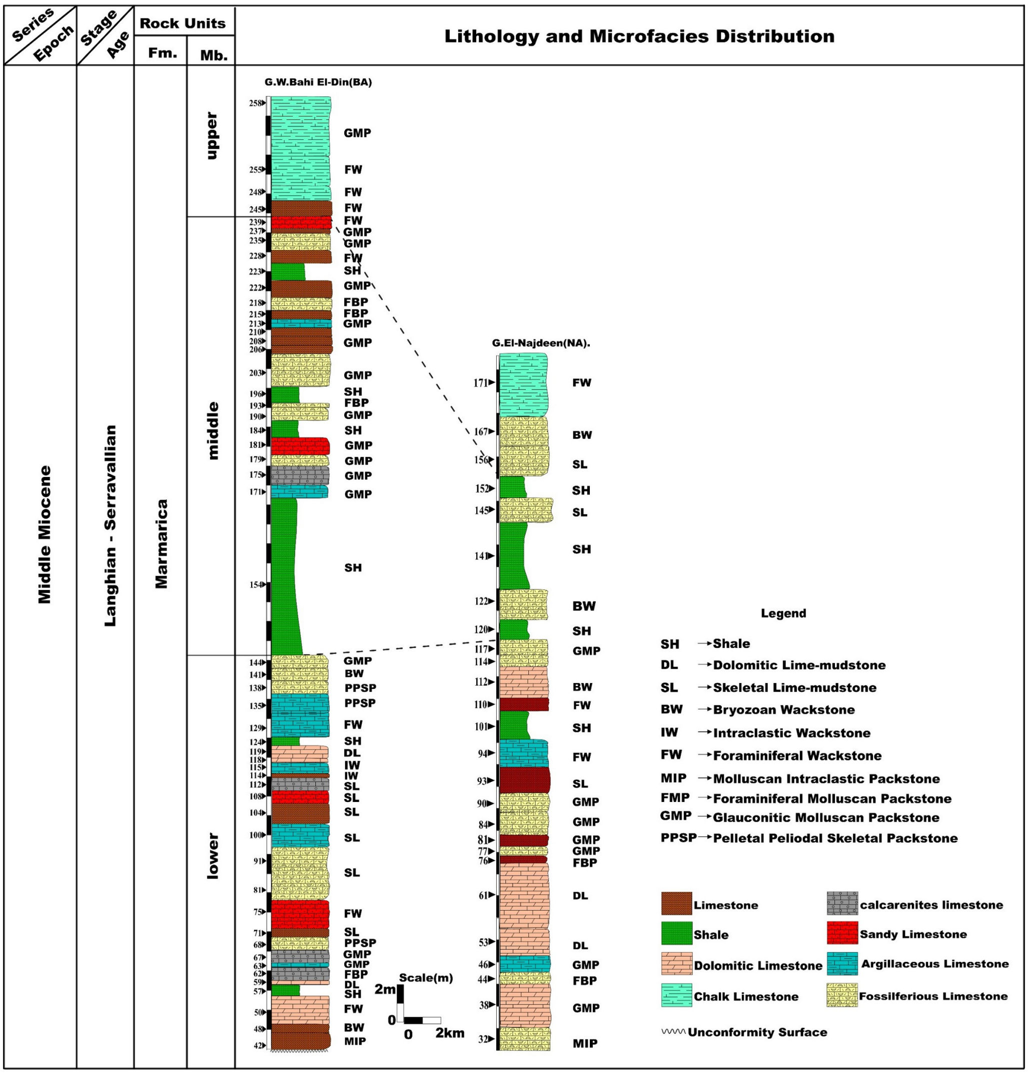

Figure 2. Lithostratigraphy and microfacies types of the Marmarica Formation at this study sections, Siwa Oasis, north western Desert (Egypt).

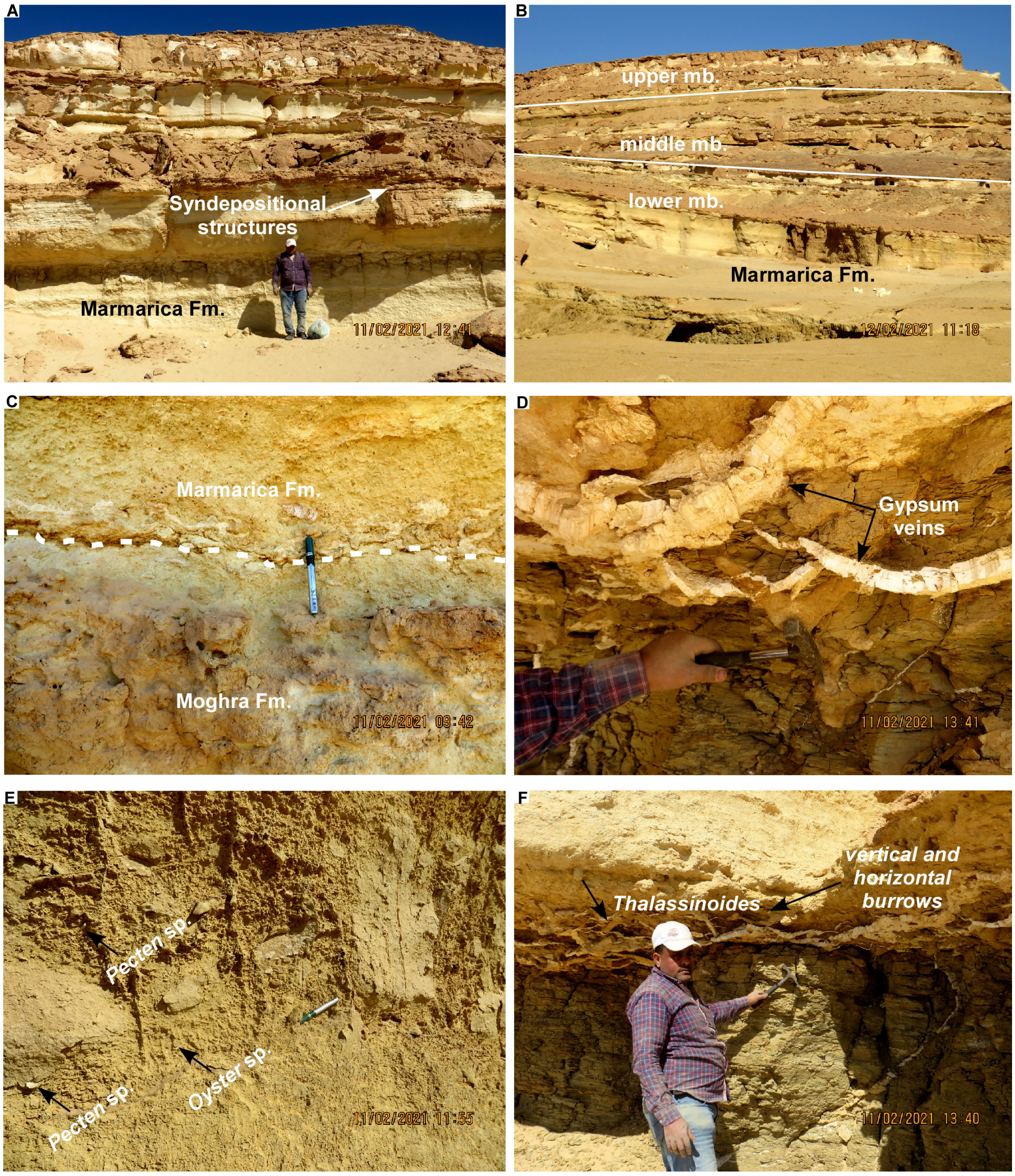

Figure 3. Field photographs show: (**A**) Stratigraphic succession of the Marmarica Fm. at Gabal Western Bahi El-Din, Siwa Oasis, with Syndeposition structure in its lower member. (**B**) Stratigraphic succession of the Marmarica Fm. at Gabal El-Najdeen, Siwa Oasis. (**C**) The sharp and uneven contact between the Moghra Formation and the Marmarica Formation at Gabal, Western Bahi El-Din. (**D**) Veins of gypsum within a shale bed at Gabal El-Najdeen. (**E**) Shell fragments of pelecypod (Bank of Pecten and Oyster) at Gabal, Western Bahi El-Din. (**F**) Vertical and horizontal burrows (*Thalassinoides*) filled with lime mud at Gabal El-Najdeen.

Figure 4. Field photographs show: (**A**) shell fragments of pelecypods (Pecten bank) at Gabal Western Bahi El-Din. (**B**) Vertical and horizontal burrows (*Thalassinoides*) filled with lime mud overlain by thick fossiliferous limestone (bank of Oyster) at Gabal Western Bahi El-Din. (**C**) Thin-bedded sandy limestone contains gypsum veins, *Oyster* sp., and gastropod casts at Gabal Western Bahi El-Din. (**D**) Bioturbated limestone overlain compact calcareous shale and veins of gypsum at Gabal, Western Bahi El-Din. (**E**) Thin laminated shale bed at the middle member at Gabal Western Bahi El-Din. (**F**) Limestone nodules in a shale bed at Gabal Western Bahi El-Din.

5.1.2. The Middle Member

It is correlative to the Siwa Escarpment member of [14]. It is about 21.3 m and 8 m thick at the Gabal Western Bahi El-Din and Gabal El-Najdeen sections, respectively (Figure 2). It consists of yellowish white, yellow, and white fossiliferous limestones interbedded with sandy limestones, argillaceous marley fossiliferous limestone, and shale at the Gabal Western Bahi El-Din and Gabal El-Najdeen (Figure 2). The limestone is yellow, reddish yellow, yellowish white and white, glauconitic, gypseous, argillaceous, marley, hard, massive, sandy, thin-bedded, bioturbated, and fossiliferous (Figure 4B–D). Macrofossils include pelecypods (*Pecten* sp. and *Oyster* sp.) as well as gastropods (Figure 4A–C). The limestone in this member is distinguished by the presence of vertical and horizontal burrows of *Thalassinoides* (Figure 4B,C). The shales in this member are light green, dark green, yellow, and yellowish green, laminated, occasionally stained with yellow color, moderately compact, soapy, highly fractured, jointed, highly calcareous, and contain bands and veins of gypsum as well as limestone nodules (Figure 4E,F).

5.1.3. The Upper Member

This member correlates with the EL-Diffa Plateau member of [14]. In this study, it constitutes the main conspicuous feature of the Marmarica Formation. It is 5.5 m and 5.4 m thick at Gabal El Najdeen and Gabal western Bahi El-Din sections, respectively (Figure 2). It consists of white to yellowish white, massive, sandy, and glauconitic chalky limestone. Chalky limestone is enriched with gastropods and pelecypods (*Oyster* sp.). At Gabal Western Bahi El-din, this member is a massive, bold-like wall that weathers to a light brown color, whereas at Gabal EL-Najdeen, it is represented by two superimposed massive beds (Figure 3A,B).

5.2. Microfacies Analysis

The microscopic investigation of the Marmarica Formation led to the recognition of nine (9) microfacies types, as represented by Table 2.

Table 2. The description of the identified microfacies of the Middle Miocene Marmarica Formation at this study sections, Siwa Oasis, northwestern Desert (Egypt).

Epoch	Rock Units	Facies Types	Occurrences	Microfacies Description
Middle Miocene	Marmarica Fm.	(1) Dolomitic lime mudstone	lower member of G. W. Bahi El-Din and G. El-Najdeen	It is composed of echinod plates (2%), elongated gastropod (1%), shell fragment of pelecypod (1%), red algae (1%), with intraclastic of subrounded lime mudstone (1%) and scattered quartz grains (1%) embedded in a dolomitic lime mud (93%).
		(2) Skeletal lime mudstone	lower member of G. W. Bahi El-Din and lower, middle, and upper members of G. El-Najdeen	It consists of glauconite patches (2 %), Foraminifera (1%), shell fragment of pelecypod (1%), bryozoa (2%), and scattered quartz grains (3%) embedded in a dark micrite ground mass (92 %).
		(3) Intraclastic wackestone	lower member of G. W. Bahi El-Din	It is composed of intraclastic (10%), glauconite (5%), gastropod (2%), and other skeletal parts and scattered quartz grains (10%) embedded in a micrite ground mass (73%).
		(4) Bryozoan wackestone	lower member of G. W. Bahi El-Din and lower, middle, and upper members of G. El-Najdeen	It consists of bryozoa (15%), echinoderms (10%), mollusca (5%), detrital quartz (5%), foraminifera (2%), ooids (1%), with glauconite patches in a micrite ground mass (63%).
		(5) Foraminiferal wackestone	lower, middle, and upper members of G. W. Bahi El-Din and lower and upper members of G. El-Najdeen	It is made up of skeletal particles and non-carbonate particles. Skeletal particles are represented by foraminifera (10%), echinoderms (10%), molluscan (5%), bryozoa (2%), ostracods (2%), with micritized pellets (2%) intraclastic (2%). Non carbonates are represented by quartz (2–3%), with gypsum replacing lime mudstone which filling most of fossils, all particles are embedded in ground mass micrite (64%).

Table 2. *Cont.*

Epoch	Rock Units	Facies Types	Occurrences	Microfacies Description
Middle Miocene	Marmarica Fm.	(6) Foraminiferal bryozoan packstone	lower and middle members of G. W. Bahi El-Din and lower member of G. El-Najdeen	It consists of skeletal particles and non-carbonate particles. Skeletal particles are bryozoa (20%), echinoderms (10%), foraminifera (10%), molluscan (5%), algae (3%), ostracods (5%), with intraclastic (3%). Non carbonate particles are quartz (3–5%), with gypsum and glauconitic patches replacing lime mudstone which filling most of fossils, these framework components are tightly packed and cemented by a mosaic of sparry calcite (39%).
		(7) Glauconitic molluscan packstone	lower, middle, and upper members of G. W. Bahi El-Din and lower member of G. El-Najdeen	It is composed of skeletal particles and non-carbonate particles. Skeletal particles are molluscan (10–15%), echinoderms (10%), bryozoa (10%), foraminifera (10%), algae (3%), coral (3%), ostracods (2%). Non carbonate particles are quartz (3–4%), with gypsum and glauconitic patches replacing lime mudstone which filling most of fossils, these framework components are tightly packed and cemented by a mosaic of sparry calcite (43%).
		(8) Molluscan intraclastic packstone	lower member of G. W. Bahi El-Din and G. El-Najdeen	It consists mainly of intraclastic (55%), mollusca (15%), echinoderms (5%) and detrital quartz grains (5%). All microfacies embedded in micrite (20%).
		(9) Pelletal peloidal skeletal packstone	lower member of G. W. Bahi El-Din	It consists of peloids (40%), molluscan (5%), ostracod (5%), echinoderms (5%), foraminifera (5%), pellets (2%), detrital quartz (5–6%), all particles embedded in micrite (42%).

5.2.1. Lime-Mudstone Microfacies (LM)

Lime-mudstone occurs in the two sections and represents 14.7% and 25.5% of the total thicknesses of the Marmarica Formation in the two studied sections. It is only present in the lower member of the Marmarica Formation at Gabal Western Bahi El-Din and in all members of Gabal El-Najdeen (Figure 2). The beds of this microfacies are yellow, brownish-yellow, and greenish-yellow, sandy, argillaceous, massive, and hard. It is from 0.2 m to 3 m thick at the lower member of Gabal Western Bahi El-Din and 4.3 m, 1.2 m, and 2.6 m at the lower, middle, and upper members of Gabal El-Najdeen, respectively. This rock consists of micron-sized micrite with sparse skeletal particles (Figure 5A).

Dolomitic Lime-Mudstone Microfacies (DL)

This microfacies was recorded in the lower members of two sections, and it represents 37.3% of the total examined lime mudstone association. This microfacies is 1.4 m thick at the lower member of Gabal Western Bahi El-Din and 4.3 m thick at the lower member of Gabal El-Najdeen (Figure 2). It is characterized by yellowish-white to white, yellow and greenish-yellow, massive, and fossiliferous rocks. Petrographically, this microfacies is composed of plates of echinoderms (2%), elongated gastropods (1%), shell fragments of pelecypods (1%), red algae (1%), intraclastic subrounded lime mudstone (1%), and scattered quartz grains (1%) embedded in dolomitic lime mud (93%, Figure 5B). Scattered quartz grains are fine, angular to subangular, moderately sorted grains. Groundmass is represented by rhomb's crystals of dolomitic lime mud, which changed into microspar due to aggrading neomorphism with many numbers of fine rhomb's crystals of dolomite. Most fossils are micritized by lime mud and replaced partially by glauconite.

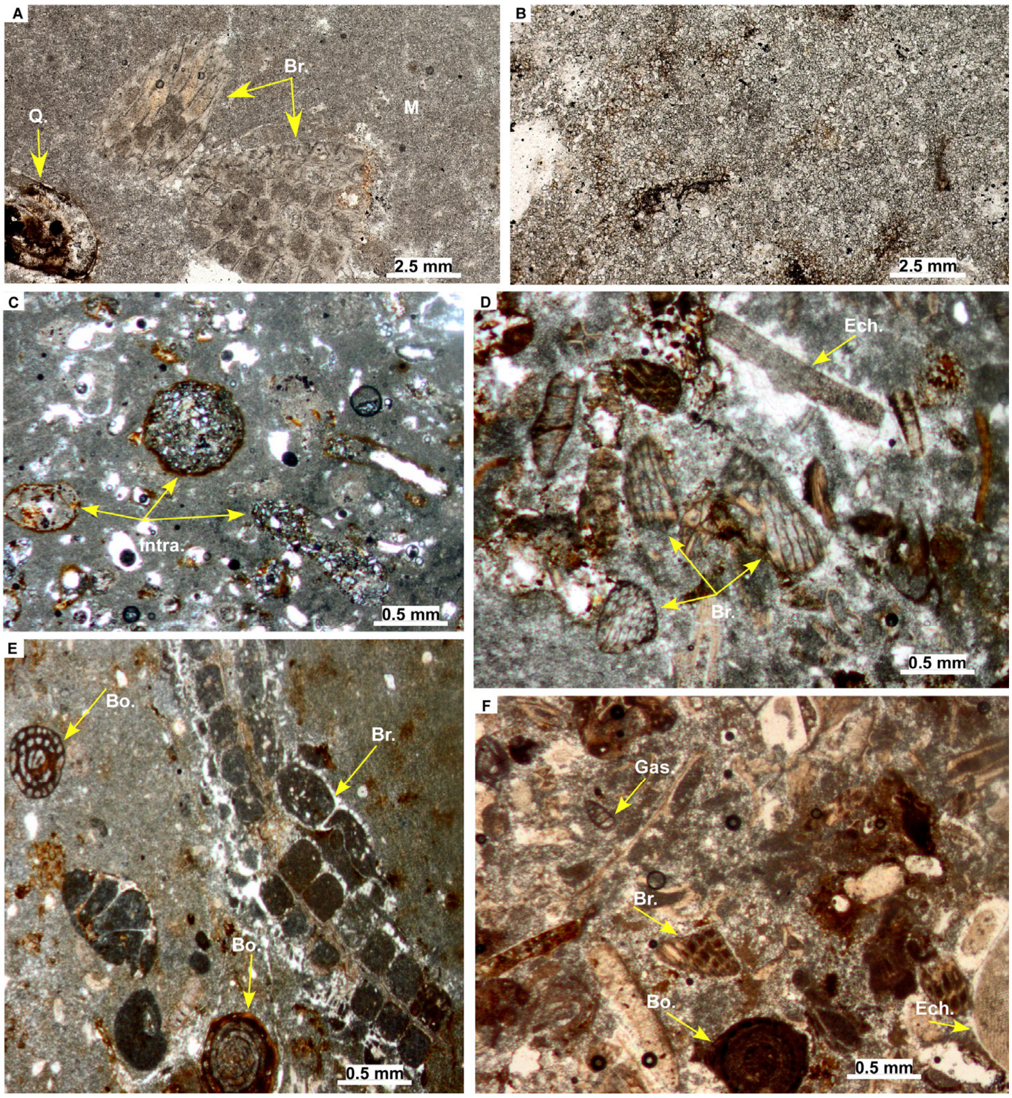

Figure 5. Thin-section photographs under Plain Polarized Light showing: (**A**) Skeletal lime-mudstone microfacies, micritized bryozoa (Br.), benthic foraminifera *Quinqueloculina* (Q.) embedded in micrite (M.), bed 12, fossiliferous limestone, lower member, Marmarica Formation, Gabal Western Bahi El-Din section. (**B**) Dolomitic lime-mudstone microfacies, bed 19, dolomitic limestone, lower member, Marmarica Formation, Gabal Western Bahi El-Din section. (**C**) Intraclastic wackestone microfacies, contains intraclastic grains (Intra.), bed 17 limestone, lower member, Marmarica Formation, Gabal Western Bahi El-Din section. (**D**) Bryozoan wackstone microfacies, bryozoa (Br.) are the dominant component in this microfacies, and tabular echinoderms (Ech.), bed 25, fossiliferous limestone, lower member, Marmarica Formation, Gabal Western Bahi El-Din section. (**E**) Foraminiferal wackstone microfacies, benthic foraminifera *Borelis melo* (Bo.), micritized bryozoa (Br), bed 50, chalky limestone, upper member, Marmarica Formation, Gabal Western Bahi El-Din section. (**F**) Foraminiferal bryozoan packstone microfacies, benthic foraminifera *Borelis melo* (Bo.), echinoderms (Ech.), surrounded by syntaxial calcite overgrowth cement (red row), Turritella gastropod (Gas.), and Bryozoa (Br.), bed 41, limestone, middle member, Marmarica Formation, Gabal Western Bahi El-Din section.

Skeletal Lime-Mudstone Microfacies (SL)

This microfacies was recorded in the lower member of Gabal Western Bahi El-Din and in the lower, middle, and upper members of Gabal El-Najdeen. It is 5.8 m thick at the lower member of Gabal Western Bahi El-Din and 1.2, 1.2, and 1.4 m thick at the lower, middle, and upper members of Gabal El-Najdeen, respectively (Figure 2). The rock of this microfacies is characterized by yellowish-white to white, yellow, dark yellow, and greenish yellow in color, is slightly fossiliferous, and is massive. Petrographically, these microfacies consist of patches of glauconite (2%), foraminifera (1%), shell fragments of pelecypod (1%), bryozoa (2%), and scattered grains of quartz (3%) embedded in a dark micrite groundmass (92%; Figure 5B). The glauconite patches are pale-yellow and green in color and replace the lime mudstone that fills the most fossils. Detrital grains of quartz are fine- to medium-grained (ranging from 0.2 mm to 0.8 mm), angular, and moderately sorted. The groundmass is represented by micrite, which changed into microspar due to aggrading neomorphism. Most fossils are micritized.

5.2.2. Wackestone Microfacies

The wackstone microfacies associations are encountered in the lower and upper members of Gabal Western Bahi El-Din and in the lower, middle, and upper members of Gabal El-Najdeen. These microfacies represent 23.4% and 30.3% of the total thickness of the Western Bahi El-Din and El-Najdeen sections, respectively (Figure 2). It includes bryozoan wackestone, intraclastic wackestone, and foraminiferal wackestone (Figure 2).

Intraclastic Wackstone Microfacies (IW)

Intraclastic wackstone microfacies occurred in the lower member of Gabal Western Bahi El-Din. These microfacies represent 8.5% of the total examined wackstone microfacies association. It measures 1.8 m at the lower member of Gabal Western Bahi El-Din (Figure 2). The bed of this microfacies is characterized by being yellowish-white to white, yellow in color, slightly fossiliferous, moderately hard, and massive. Under a microscope, these microfacies are made up of intraclastic (10%), glauconite (5%), gastropod (2%), and other skeletal parts, as well as scattered grains of quartz (10%) included in a groundmass of micrite (73%, Figure 5C). Intraclastic grains are rounded, subrounded lime mud filled with fine quartz grains. The glauconite plates are pale-yellow in color, and they show partial and complete replacement of lime mudstone (micrite) with a random distribution. Detrital grains of quartz are characterized by fine (ranging from 0.1 mm to 0.2 mm), angular to subangular, and moderately sorted grains. The cementing material is represented by micrite, which changed into microsparite due to aggrading neomorphism. Most fossils are micritized and recrystallized to microspar size.

Bryozoan Wackestone Microfacies (BW)

Bryozoan wackestone microfacies are recorded in the lower member of Gabal Western Bahi El-Din and in the lower, middle, and upper members of Gabal El-Najdeen (Figure 2). It is 1.2 m and 4.8 m thick at Gabal Western Bahi El-Din and Gabal El-Najdeen, respectively (Figure 2). It represents 28.5% of the total examined wackstone associations. The rocks of these microfacies are characterized by being yellowish- white, white to reddish-yellow in color, massive, sandy, slightly argillaceous, and highly fossiliferous (Figure 2). Petrographically, it consists of bryozoa (15%), echinoderms (10%), mollusca (5%), detrital quartz (5%), foraminifera (2%), ooids (1%), and glauconite patches in a micrite ground mass (63%, Figure 5D). The bryozoan chambers are filled with lime mud that changes into neomorphic sparite. Mollusca shell fragments are represented by gastropod and pelecypod shell fragments. Turritella gastropod chambers are filled with glauconite and pelecypod shell fragments and show random distribution in the rock. Echinoderms occur in the form of tabular plates. Foraminifera are represented by *Borelis melo* and *Quinqueloculina* sp. Grains of quartz are characterized by being fine to medium, monocrystalline, subrounded, moderately sorted, and scattered randomly in the microfacies. Shell fragments of fossils were partially micritized, while little of these fossils were originally kept in aragonitic fabric. Glauconite patches are pale-green to pale-yellow. The cement is represented by micrite, which changed into microspar due to aggrading neomorphism filling the cavities among the main constituents.

Foraminiferal Wackstone Microfacies (FW)

Foraminiferal wackstone microfacies are noted in the lower, middle, and upper members of Gabal Western Bahi El-Din and in the lower and upper members of Gabal El-Najdeen. It attains 8.4 m and 4.8 m thick at Gabal Western Bahi El-Din and Gabal El-Najdeen, respectively (Figure 6). It records 63.1% of the total examined wackstone associations. It is characterized by being yellowish-white to white and greenish-yellow in color, massive, and fossiliferous (Figure 6). Petrographically, it is composed of skeletal particles and non-carbonate particles. Skeletal particles are represented by foraminifera (10%), echinoderms (10%), molluscan (5%), bryozoa (2%), ostracods (2%), micritized pellets (2%), and intraclastic (2%). Non-carbonate particles are represented by quartz (2–3%), gypsum replacing lime mudstone that fills most fossils. All particles are embedded in micrite groundmass (64%, Figure 5E). Foraminifera is represented by *Borelis melo* and *Quinqueloculina* sp. Echinoderms are rounded, tabular plates. Mollusca is represented by shell fragments of pelecypods and gastropods. Grains of quartz are fine to medium, monocrystalline, subrounded, and moderately sorted. Its size reaches 0.5 mm. Intraclastics are subrounded to rounded lime mud. Shell fragments are partially and completely recrystallized to microsparite or micrite, while few of these fossils were originally preserved in aragonitic texture. The cementing material is represented by micrite, which changed into microsparite due to aggrading neomorphism filling the cavities among the main constituents.

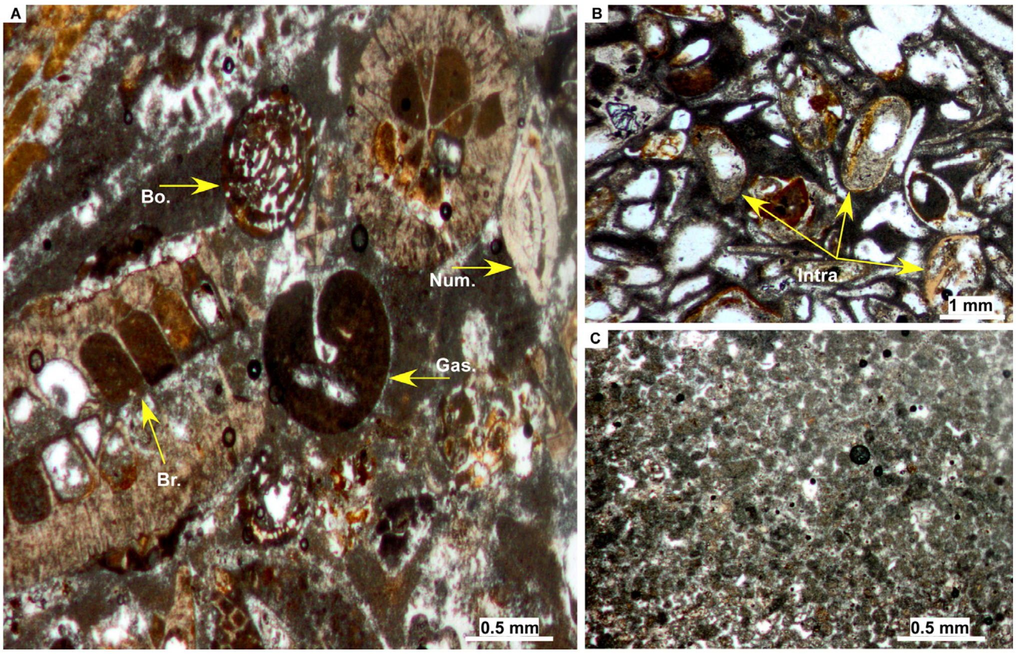

Figure 6. Thin-section photographs under Plain Polarized Light showing: (**A**) Glauconitic molluscan packstone microfacies, benthic foraminifera *Borelis melo* (Bo.), reworked *Nummulites* (Num.), gastropods (Gas.), and Bryozoa (Br.), bed 17, fossiliferous limestone, the lower member, Marmarica Formation, Gabal El-Najdeen section. (**B**) Intraclastic Molluscan packstone microfacies, intraclastic grains of lime-mudstone with shell fragments of mollusca, bed 1, fossiliferous limestone, the lower member, Marmarica Formation, Gabal El-Najdeen section. (**C**) Pelletal peloidal skeletal packstone microfacies consist of micritized peloids (Pel.) embedded in micrite, bed 23, argillaceous limestone, the lower member, Marmarica Formation, Gabal Western Bahi El-Din section.

5.2.3. Packstone Microfacies Association

This member correlates with the EL-Diffa Plateau Member of [14]. It constitutes the main conspicuous feature of the Marmarica Formation in this study. It is 5.5 m and 5.4 m thick at the Gabal El-Najdeen and Gabal Western Bahi El-din sections, respectively (Figure 2). It consists of white to yellowish-white, massive, sandy, and glauconitic chalky limestone. Chalky limestone is enriched with gastropods and pelecypods (*Oyster* sp.). At

Gabal Western Bahi El-din, this member is a massive, bold-like wall that weathers to a light brown color, whereas at Gabal El-Najdeen, it is represented by two superimposed massive beds.

Foraminiferal Bryozoan Packstone Microfacies (FBP)

Foraminiferal bryozoan packstone microfacies are encountered in the lower and middle members of Gabal Western Bahi El-Din and the lower member at Gabal El-Najdeen (Figure 2). It measures 1.8 m and 0.6 m thick at the Gabal Western Bahi El-Din and Gabal El-Najdeen, respectively. It represents 9.6% of the total examined packstone associations. It is yellow to brownish-yellow, yellowish-white to white, and yellow in color. It is massive, sandy, glauconitic, ferruginous, and fossiliferous. Petrographically, the (FBP) microfacies are composed of skeletal particles and non-carbonate particles. Skeletal particles are represented by bryozoa (20%), echinoderms (10%), foraminifera (10%), molluscans (5%), algae (3%), ostracods (5%), and intraclastics (3%). Non-carbonate particles are represented by quartz (3–5%), with gypsum and glauconitic patches replacing lime mudstone, which fills most of the fossils (Figure 5F). These framework components are tightly packed and cemented by a mosaic of sparry calcite (39%). Mollusca is represented by a shell fragment of a pelecypod, and gastropods are randomly distributed in the thin section. Foraminifera is represented by *Borelis melo* and *Quinqueloculina* sp. The echinoderm's debris is rounded and tabular. Intraclastic is rounded to sub-rounded lime-mudstone. Chambers of bryozoa and foraminifera are filled with lime mud. Detrital grains of quartz are characterized by fine to medium, monocrystalline, subrounded, and moderately sorted grains, and they reach 0.6 mm in size. Most fossil fragments have their original fibrous structure; while a few of them are recrystallized to sparry calcite, a few mollusca shell fragments were originally preserved in an aragonitic texture. The cementing material is micrite, which changed into microspar due to aggrading neomorphism and is filling the cavities among the main constituents.

Glauconitic Molluscan Packstone Microfacies (GMP)

This microfacies is recognized in the lower, middle, and upper members of Gabal Western Bahi El-Din and in the lower member of Gabal El-Najdeen (Figure 6). It measures 9.4 m and 3.6 m thick at the Gabal Western Bahi El-Din and Gabal El-Najdeen, respectively (Figure 6). It represents 52% of the total examined packstone associations. The beds of this microfacies are characterized by being yellow, dark brownish-yellow, yellowish-white, and white in color, massive, sandy, glauconitic, and highly fossiliferous. Petrographically, it is composed of skeletal particles and non-carbonate particles. Skeletal particles are represented by molluscan (10%–15%), echinoderms (10%), bryozoa (10%), foraminifera (10%), algae (3%), coral (3%), and ostracods (2%). Non-carbonate particles are represented by quartz (3%–4%), with gypsum and glauconitic patches replacing lime mudstone, which fills most of the fossils. These framework components are tightly packed and cemented by a mosaic of sparry calcite (43%; Figure 6A). Mollusca is represented by shell fragments of pelecypods and gastropods. Foraminiferal taxa are represented by *Borelis melo* and *Quinqueloculina* sp., and their chambers are filled with lime mud. The echinoderm's debris is rounded and tabular. Chamber of bryozoa filled with glauconitic lime mud. Grains of quartz are fine, monocrystalline, angular, and moderately sorted grains. The majority of the fossil remains exhibit their original fibrous structure, while a few of them are recrystallized into sparry calcite. A few mollusca were originally preserved in aragonitic texture. The cementing material is represented by micrite, which changed into microspar due to aggrading neomorphism filling the cavities among the main constituents.

Molluscan Intraclastic Packstone Microfacies (MIP)

This microfacies is encountered in the lower member of the Marmarica Formation of the studied sections. It attains 0.8 m and 1.2 m thick at the Gabal Western Bahi El-Din and Gabal El-Najdeen, respectively (Figure 2). It represents 8% of the total examined wackstone associations. Its rocks are characterized by being yellowish-white to white and reddish-yellow in color, massive, slightly argillaceous, gypseous, and fossiliferous (Figure 2). Petrographically, it consists mainly of intraclastics (55%), mollusca (15%), echinoderms (5%), and detrital quartz grains (5%). All these particles are embedded in micrite (20%, Figure 6B). Quartz grains are fine to medium, angular to subrounded, monocrystalline, exhibit unit extinction, and are moderately sorted. Most shell fragments of mollusca are completely or partially micritized with lime mud and recrystallized into microspar, while a few of them were originally kept in aragonitic texture. Echinoderms are represented by spiny forms. The intraclasts are mainly represented by lime-mudstone clasts. These clasts are subrounded and surrounded by microcrystalline calcite. The cementing material is composed of dark gray lime mudstone, and parts of this lime mud have changed into microspar due to aggrading neomorphism.

Pelletal Peloidal Skeletal Packstone Microfacies (PPSP)

Peloids are carbonate grains that are round, microcrystalline, and cryptocrystalline. Under a transmitted light microscope, they appear dark, whereas they appear white in direct light [35]. It is only encountered in the lower member of Gabal, Western Bahi El-Din. It measures 1.4 m thick (Figure 2). It represents 5.6% of the total examined packstone associations. The rocks of these microfacies are characterized by being yellow and yellowish-white to white in color, massive, sandy, glauconitic, ferruginous, and fossiliferous. In thin sections, it consists of peloids (40%), molluscan (5%), ostracod (5%), echinoderms (5%), foraminifera (5%), pellets (2%), and detrital quartz (5%–6%). All particles are embedded in micrite (42%; Figure 6C). Mollusca is represented by shell fragments of pelecypods, which show random distribution, and *Turritella* gastropods, which are filled with glauconitic lime mud. Some molluscan shells are micritized and recrystallized into microsparite, and some of them keep their original aragonitic texture. The debris of echinoderms is tabular and spiny in shape. Foraminifera is represented by *Borelis melo* and *Quinqueloculina* sp., and their chambers are filled with gypseous lime mud. Ostracods are micritized with gypseous lime mud. Grains of quartz are fine to medium monocrystalline grains, angular to surrounded, moderately sorted grains that exhibit unit extinction, and their size ranges from 0.2 mm to 0.4 mm. Peloids are micritized with lime mud, and their size ranges from 0.3 mm to 0.6 mm. The cementing material is represented by micrite, which changed into microspar due to aggrading neomorphism, and fills the cavities among the main constituents.

5.2.4. Claystone Lithofacies

This lithofacies has a wide distribution in the Marmarica Formation. It is intercalated with limestone. It ranges in thickness from 0.4 m to 8 m. It has a total thickness of 11.2 m and 6.8 m at the Gabal Western Bahi El-Din and Gabal El-Najdeen, respectively (Figure 2). It usually occurs at the basal part of the shallowing-upward cycles. The claystone is green to yellowish green, laminated, and contains thin laminae of gypsum. Such claystone usually contains disconnected lenses of marly limestone and smaller, lenticular to ellipsoidal marly limestone (Figure 4E,F). Some samples of claystone were analyzed by X-ray diffraction to determine the types of clay minerals. It is noticed that few samples contain dolomite and kaolinite (Figure 7A–C), whereas the majority of claystone beds include kaolinite and montmorillonite (Figure 7D–F).

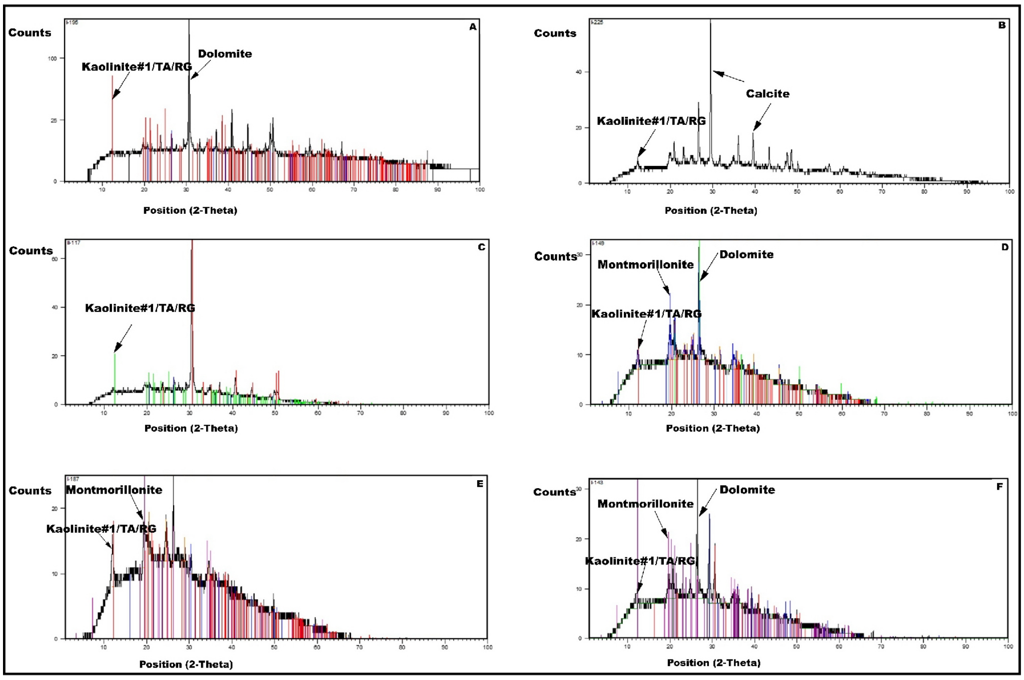

Figure 7. X-ray diffraction pattern of clay fraction: (**A**) Sample 195, bed 35, the middle member, Marmarica Formation, Gabal Western Bahi El-Din; (**B**) Sample 225, bed 44, the middle member, Marmarica Formation, Gabal Western Bahi El-Din; (**C**) Sample 117, bed 19, the middle member, Marmarica Formation, Gabal El-Najdeen; (**D**) Sample 149, bed 27, the middle member, Marmarica Formation, Gabal Western Bahi El-Din; (**E**) Sample 187, bed 32, the middle member, Marmarica Formation, Gabal Western Bahi El-Din; (**F**) Sample 143, bed 21, the middle member, Marmarica Formation, Gabal El-Najdeen.

5.2.5. Dolostone

The dolostones have been found in the lower member of the Marmarica Formation in the studied sections. It attains 2.8 m and 7.3 m thick at the Gabal Western Bahi El-Din and Gabal El-Najdeen, respectively (Figure 2). Petrographic properties of the dolomites were examined by scanning electron microscopy (SEM) and a thin section under a polarizing microscope. Following [36–38], the textures of dolomite are subdivided depending on the distribution of crystal size and the shape of the crystal boundary (Figure 8). The following textures were recognized in this study:

Unimodal, Fine-Crystalline Planar-e (Euhedral)

It is composed of unimodal, fine planer-e euhedral crystals (18.4 µm–22.1 µm) showing mosaic textures. Mosaics are mostly planar-e crystals and finely crystalline. The crystals may have clear or cloudy textures. The relatively fine crystals of these dolomites are clean, with faint inclusions and the absence of zoning. This type is characterized by intercrystalline pore spaces. Textures have no replacement and have porous, intercrystalline areas. This type of dolostone was recorded in the lower member of the Marmarica Formation at the Gabal Western Bahi El-Din and Gabal El-Najdeen sections (Figure 8A,B).

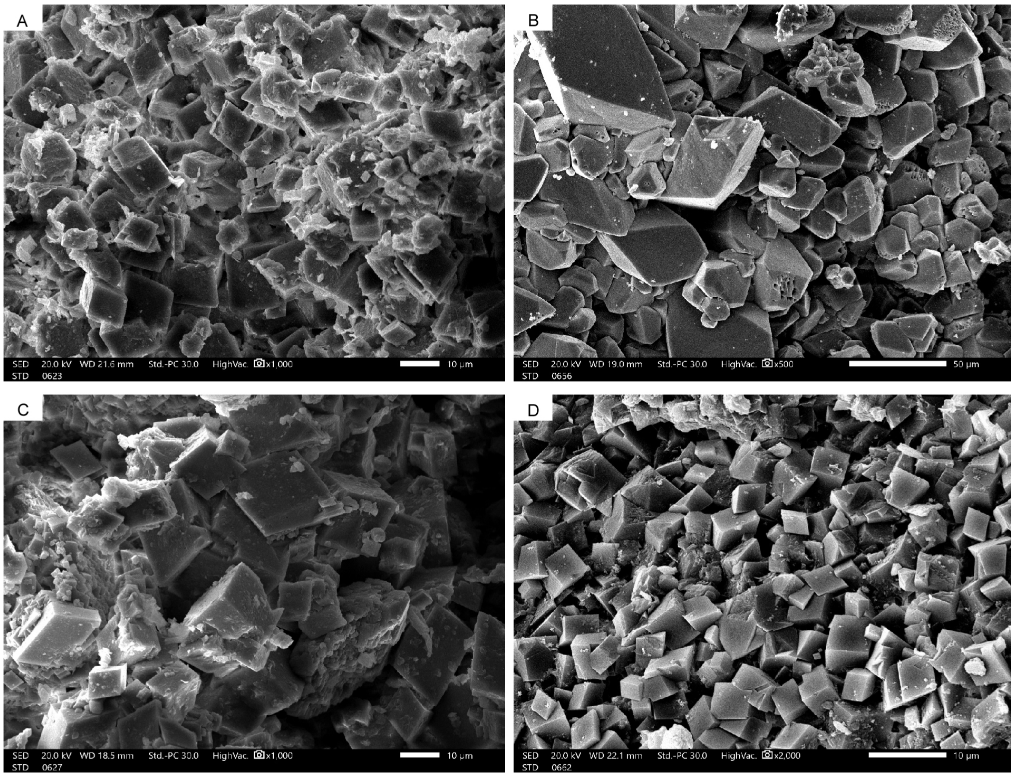

Figure 8. SEM images illustrate: (**A**) Unimodal, fine-crystalline planar-e(euhedral) matrix of dolomite from glauconitic sandy skeletal wackestone microfacies, bed 3, the lower member, Marmarica Formation, Gabal Western Bahi El-Din. (**B**) Unimodal, fine-crystalline planar-e (euhedral) crystals, dolomitic lime-mudstone microfacies, bed 6, the lower member, Marmarica Formation, Gabal El-Najdeen. (**C**) Fine, subhedral rhombic dolomite crystals from dolomitic lime-mudstone microfacies, bed 19, the lower member, Marmarica Formation, Gabal Western Bahi El-Din. (**D**) Polymodal, Euhedral rhombic dolomite crystals, dolomitic lime-mudstone microfacies, bed 20, the lower member, Marmarica Formation, Gabal Western Bahi El-Din.

Polymodal, Fine-Crystalline Planar-s (Subhedral)

It is composed of fine, planer-s subhedral crystals (19 µm) showing mosaic textures. Mosaics are mostly planar-s crystals and finely crystalline dolomite. The crystals may have clear or cloudy textures. The fine crystals of dolomites are clean, with faint inclusions and no zoning. This type of dolomite is characterized by being polymodal with abundant intercrystalline pore spaces. Textures have no replacement and have porous, intercrystalline areas. This type of dolostone was found in the lower member of the Marmarica Formation at the Gabal Western Bahi El-Din section (Figure 8C,D).

5.3. The Cyclicity

Cyclicity is related to sea level fluctuations [39–50]. The current study used the term emergence, which means regressive or shallowing-upward cycles, to describe the cyclicity in the Marmarica Formation [48]. These cycles consist of pure carbonates and mixed siliciclastic carbonates. Each cycle begins with clay and is capped by limestone (Figure 9). These cycles can be classified into gradual and non-gradual cycles as follows:

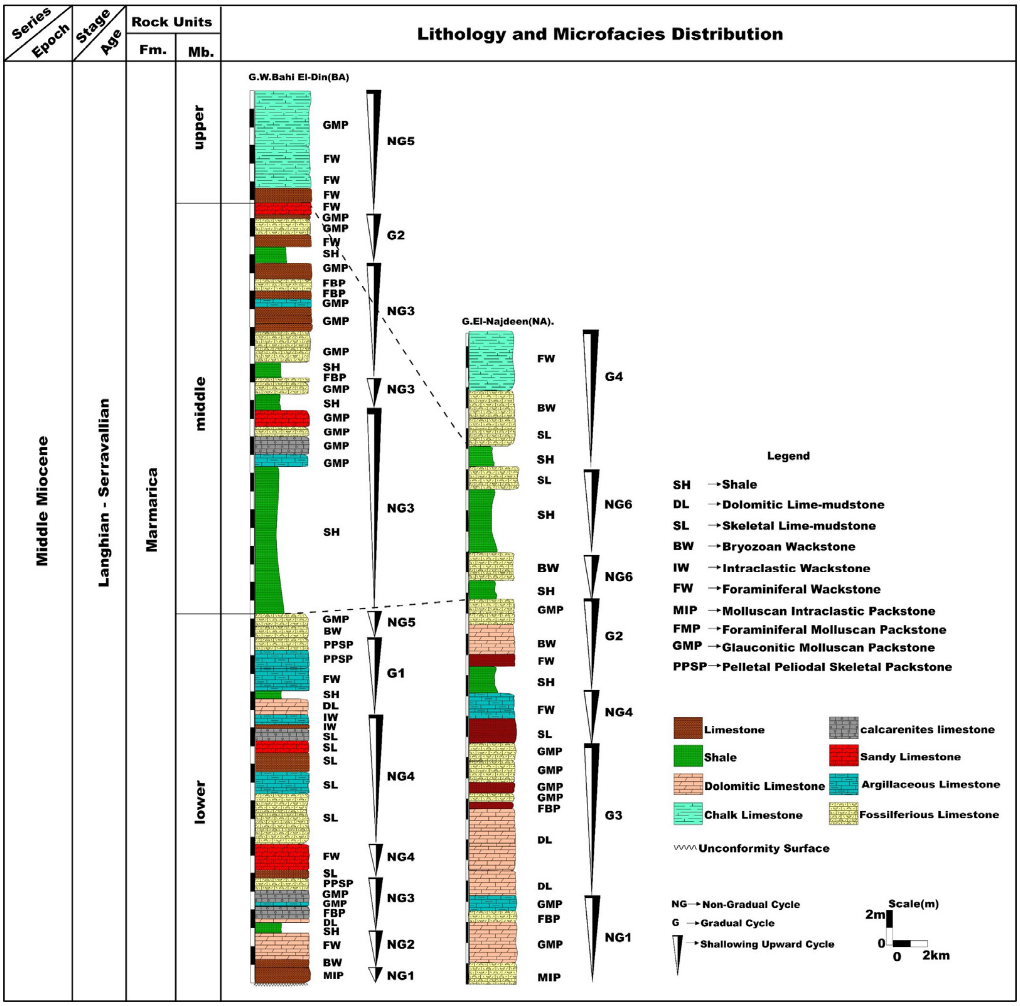

Figure 9. Lithostratigraphy and different microfacies of the Marmarica Formation are coupled with the vertical arrangement of their shallowing-upward cycles at the two studied sections.

5.3.1. The Gradual Cycles

It describes the progressive change from one habitat to another. The change might be shallowing upward or deepening upward; however, there is no remarkable unexpected facies variation from shallow to deep [48]. Four types of gradual cycles (G1, G2, G3, and G4) were recognized in the Marmarica Formation in the studied sections (Figure 9).

The Gradual Cycle Type 1 (G1)

It was found in the lower member of the Marmarica Formation at the Gabal Western Bahi El-Din section (Figure 9). Each cycle has a range thickness of about 2.4 m. It consists of mixed clastic-carbonate sediments. It begins with dolomitic lime-mudstone (1.2 m) overlain by shale (0.4 m) at the base, followed by foraminiferal wackestone (1.2 m) in the middle and capped by pelletal peloidal skeletal packstone (0.8 m) at the top (Figure 10A(a),B).

The Gradual Cycle Type 2 (G2)

It is encountered in the lower member of the Marmarica Formation at Gabal El-Najdeen and in the upper member of the Marmarica Formation at Gabal Western Bahi El-Din (Figure 9). At Gabal Western Bahi El-Din, this type consists of shale (1 m), is overlain by deep subtidal foraminiferal wackestone (1.8 m), and is capped by shallow subtidal facies glauconitic and molluscan packstone (0.6 m; Figure 10A(b),C). At Gabal El-Najdeen, it consists of shale (1.2 m) overlain by foraminiferal wackestone (0.6 m), bryozoan wackestone (1.6 m), and is capped by glauconitic molluscan packstone (1.2 m; Figure 10A(c),D).

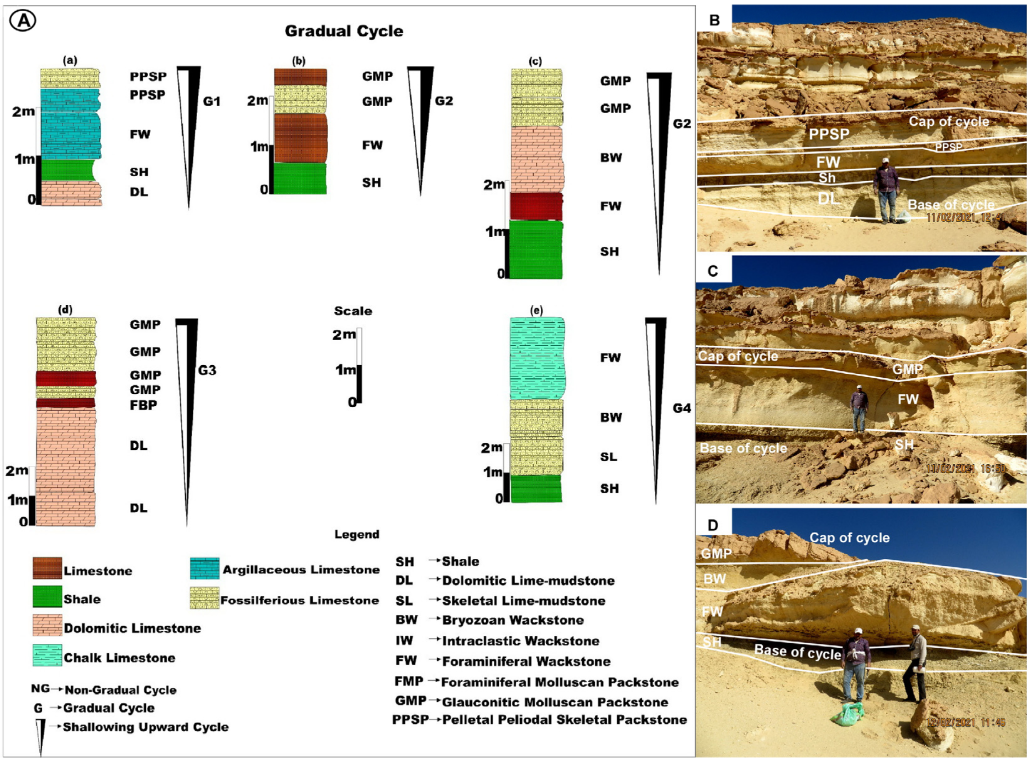

Figure 10. (**A**) The G1 (**a**), G2 (**b**,**c**), G3 (**d**), and G4 (**e**) types of gradual emergence cycles of the Marmarica Formation are described in this study sections. (**B**) A field photograph shows the first type of gradual cycle (G1) in the lower member, Gabal Western Bahi El-Din section. (**C**) A field photograph shows the second type of gradual cycle (G2) in the middle member, Gabal Western Bahi El-Din section. (**D**) A field photograph shows the second type of gradual cycle (G2) in the lower member, Gabal El-Najdeen section.

The Gradual Cycle Type 3 (G3)

It is recorded in the lower member of the Marmarica Formation at Gabal El-Najdeen (Figure 9). It consists of deep subtidal dolomitic lime mudstone (4.3) overlain by shallow subtidal foraminiferal bryozoan packstone (0.2 m) and is capped by glauconitic molluscan packstone (2 m; Figure 10A(d)).

The Gradual Cycle Type 4 (G4)

It has been found in the upper member of the Marmarica Formation at Gabal El-Najdeen (Figure 9). It consists of shale (1.4 m) overlain by skeletal lime mudstone (1.2 m), bryozoan wackestone (0.8 m), and is capped by foraminiferal wackestone (3 m; Figure 10A(e)).

5.3.2. The Non-Gradual Cycles

The Non-Gradual Cycle Type 1 (NG1)

It occurs at the lower member of the Marmarica Formation at Gabal Western Bahi El-Din and Gabal El-Najdeen (Figure 9). It consists of 0.8 m-thick molluscan intraclastic packstone at Gabal Western Bahi El-Din (Figure 11A(a)). At Gabal El-Najdeen, it consists of 4 m-thick molluscan intraclastic packstone, overlain by glauconitic molluscan packstone and foraminiferal bryozoan packstone, and is capped by glauconitic molluscan packstone (Figure 11A(b)).

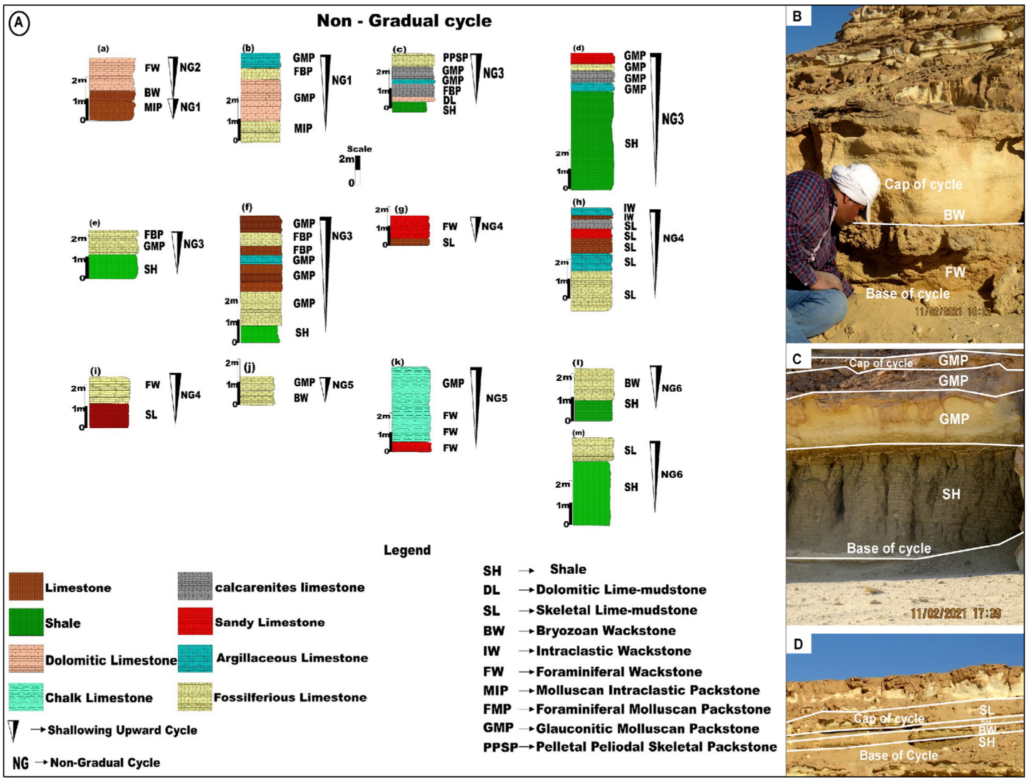

Figure 11. (**A**) The NG1 (**a**,**b**), NG2 (**a**), NG3 (**c**–**f**), NG4 (**g**–**i**), NG5 (**j**,**k**), and NG6 (**l**,**m**) types of non-gradual emergence cycles of the Marmarica Formation are described in this study sections. (**B**) A field photograph shows the NG2 type of non-gradual cycle at the lower member of the Marmarica Formation at the Gabal Western Bahi El-Din section. (**C**) A field photograph shows the NG3 type of non-gradual cycle at the middle member of the Marmarica Formation at the Gabal Western Bahi El-Din section. (**D**) A field photograph shows the NG6 type of non-gradual cycle at the middle member of the Marmarica Formation at the Gabal El-Najdeen section.

The Non-Gradual Cycle Type 2 (NG2)

It occurs only in the lower member of the Marmarica Formation at Gabal, Western Bahi El-Din (Figure 9). It consists of bryozoan wackestone (0.6 m thick) capped by 1.2 m thick foraminiferal wackestone (1.2 m thick; Figure 11A(a),B).

The Non-Gradual Cycle Type 3 (NG3)

It is noted in the lower and middle members of the Marmarica Formation at Gabal, Western Bahi El-Din (Figure 9). In the lower member, it consists of shale (0.4 m) overlain by dolomitic lime mudstone (0.2 m), foraminiferal bryozoan packstone (0.6 m), glauconitic molluscan packstone (1 m), and capped by pelletal peloidal packstone (0.8 m; Figure 11A(c)). It changes upward from deep subtidal to shallow subtidal. At the lower portion of the middle member, it consists of a thick bed of shale (8 m) overlain by glauconitic molluscan packstone (3 m; Figure 11A(d),C). At its middle part, it consists of shale (0.6 m) overlain by glauconitic molluscan packstone (1.8 m) and is topped by foraminiferal bryozoan packstone (0.2 m; Figure 11A(e)). At the upper part of the middle member, this type consists of shale (0.8 m) overlain by glauconitic molluscan packstone (3.2 m), foraminiferal molluscan packstone (0.4 m), and foraminiferal bryozoan packstone (0.6 m) and is topped by glauconitic molluscan packstone (0.8 m; Figure 11A(f)).

The Non-Gradual Cycle Type 4 (NG4)

This type is recorded in the lower member of the Marmarica Formation at Gabal Western Bahi El-Din and Gabal El-Najdeen (Figure 9). It is composed of lime mudstone and wackestone, which represent deep subtidal facies. At Gabal Western Bahi El-Din, the lower part of this member consists of skeletal lime mudstone (0.4 m) overlain by foraminiferal wackstone (1.4 m; Figure 11A(g)). In the middle part, it consists of skeletal lime mudstone (6.4 m) and is overlain by intraclastic wackestone (0.8 m; Figure 11A(h)). At Gabal El-Najdeen, this type consists of skeletal lime mudstone (1.2 m) and is capped by foraminiferal wackstone (1.2 m; Figure 11A(i)).

The Non-Gradual Cycle Type 5 (NG5)

It is found in the lower and upper members of the Marmarica Formation at Gabal, Western Bahi El-Din (Figure 9). It consists of a deep subtidal wackestone capped by shallow subtidal packstone (Figure 11A(j)). At the lower member, the base of this cycle is composed of bryozoan wackestone (0.6 m) and is topped by glauconitic molluscan packstone (0.6 m; Figure 11A(j,k). At the upper member, it consists of foraminiferal wackestone (4 m) and is capped by glauconitic molluscan packstone (3 m; Figure 11A(k)).

The Non-Gradual Cycle Type 6 (NG6)

It is recorded at the middle member of the Marmarica Formation at Gabal El-Najdeen (Figure 9). At the lower part, it consists of deep subtidal shale (1 m) overlain by deep subtidal bryozoan wackstone (2 m; Figure 11A(l)). At the upper part, it consists of shale (3.6 m) and is capped by deep subtidal skeletal lime-mudstone (1.2 m; Figure 11A(m),D).

6. Discussion

The depositional history of the Marmarica Formation was discussed by several authors [15,17,18,51–53]. This formation was deposited on a homoclinal ramp setting [16,17]. Their interpretation is based on the lack of reefs along the southern exposure in the Siwa Oasis and in the coastal outcrops at Salum. On the contrary, [22] mentioned that the Marmarica Formation includes an assemblage of invertebrate fossils and foraminifera, which indicate neritic and reefal settings.

In the current study, the (LM) microfacies were formed in a relatively calm condition in a deep subtidal zone, below the wavebase, and shielded from the current activity. This was indicated by the dominance of the abundance of fine-grained carbonates and the lack of a conclusive indicator of grain support [54]. The abundance of (DL) facies within micrite indicates that it formed in a shallow setting with quite water conditions [55]. The presence of skeletal debris such as echinoids, pelecypods, and algae suggests an open marine platform [35]. The scattered distribution of euhedral rhombs of dolomite within the lime mud indicates that local dolomitization took place at late diagenesis. The source of Mg ions needed for local dolomitization was most probably derived from the high-magnesium calcite skeletal particles. The quantity of micritic matrix within the (SL) microfacies, which includes tiny fragments of pelecypod skeleton, in the lime-mudstones shows that they were deposited in a deep subtidal environment with low energy [56,57]. The peloids of glauconite, which occur within micrites and replace the neomorphosed calcite, point to the authigenic origin of glauconite, developed on the middle shelf (shallow marine). Glauconite often has an authigenic origin, can only be found in marine environments, and is commonly associated with low levels of oxygen [58,59]. Peloids of glauconite were found as solitary pellets, which suggests a low rate of deposition. Glauconites are currently discovered on continental shelves (shallow water) [60]. According to [61], the disintegration of spongy spicules and other organisms containing silica may be the reason for the presence of microcrystalline silica.

Intraclasts within (IW) microfacies are pieces of locally sourced, early cemented limestones. Different types of rock (intraclasts, lime mud, and quartz grains) are present, which suggests that there was a transition between low- and high-energy conditions. Intraclasts show how sediments were broken up in the intertidal zone and then redeposited in the subtidal zone. Lime-mud intraclasts and detrital quartz grains are most common close to the shoreline in the intertidal as well as subtidal zones of the inner shelf restricted zone [62]. The meniscus and fine crystalline cements that surround the grains of these sediments indicate that they were impacted by vadose and meteoric fresh-water phreatic diagenesis [63]. Within the (BW) microfacies, the wackestone is associated with the shallow subtidal-intertidal zone [64]. According to [35,56], the prevalence of micrite in this lithofacies appears to imply shallow neritic water with a broad circulation regime and a low-energy subtidal open marine shelf as a depositional environment. According to [65], the bryozoans that were recorded in the Siwa Oasis resided in the littoral-sublittoral zone, where sedimentation rates were low. The fossil association of bryozoans, benthic foraminifera, oysters, pectinids, serpulids, and echinoderms indicates a shallow marine habitat. Based on [35], the widespread presence of lime mud within the (FW) microfacies suggests a low-energy depositional environment where fine matrix accumulated. Foraminiferal taxa: alveolinids, *Borelis melo*, and *Quinqueloculina* sp. are indicators of quiet water habitats [66]. The larger foraminifera reside above the depth of the euphotic zone [57]. The wackstone microfacies indicate the shallow subtidal-intertidal zone [64]. The faunal assemblages within the (FBP) microfacies may point to accumulation in a moderately to very energetic shallow marine environment. [65] mentioned that the Marmarica Formation was deposited between 20 and 60 m, based on studying the bryozoan assemblages in the Siwa Oasis.

Concerning the (GMP) microfacies, [67] documented that the glauconitic molluscan packstone was likely formed in a shallow subtidal (high energy) depositional environment. The microfacies rich in molluscan point to a shoaling habitat above the typical wavebase, which was accumulated at the shelf border dividing the open marine from the more constrained marine environment [35,56]. The abundance of typical marine fauna and carbonate mud both indicate deposition in a zone of wave agitation that is quite shallow in the marine environment [68]. The inner shelf is indicated by the association of large pelecypods [69]. Additionally, pelecypod and gastropod remains occur between 20 and 50 m beneath the surface [70]. Micritization of pelecypod shells was primarily carried out by fungi and algae in shallow, constrained sea water [71]. The glauconite grains are of allochthonous origin and were reworked from older layers, which introduced glauconite into sediments [72]. According to [73], glauconite was likely formed on the current continental shelf at depths between tens and hundreds of meters. For (MIP) microfacies, carbonates that are supported by grains and exhibit powerful water agitation are called packstones [35]. The richness of the fauna, which includes mollusca, echinoderms, and foraminifera, indicates deposition of normal salinity, well-oxygenated open marine onto the inner shelf with a depth of >30 m, and points to microfacies indicate a mid-ramp setting [71]. According to [56], the fauna that is found in the packstone microfacies implies an open shelf and typical marine conditions. The presence of micrite groundmass as well as the abundance of the remains of skeletal fauna that live in open-marine environments (e.g., echinoids, bryozoans, and foraminifera) point to an open-marine habitat with low-to-moderate energy [35,56]. Within the (PPSP) microfacies, peloids are prevalent in deep-water carbonates as well as reef and mud mound carbonates that are found in tidal and subtidal shelf settings. They are common in tropical areas that have shallow-marine carbonates and uncommon or absent in non-tropical cool water carbonates [35].

The occurrence of the claystone lithofacies at the base of the Marmarica Formation suggests transgression, followed by relatively shallowing upward and depositing the carbonate facies. The dominance of montmorillonites and kaolinite indicates a marine depositional environment [74] and shows deposition in a low-energy environment [75]. The bioturbation that characterized these facies indicates a coastal grass-flat depositional environment. The diagenesis of kaolinite commonly produces illite. Kaolinite is a product of the chemical weathering of feldspar and has a typical marine origin [76]. The lenticular carbonates are evidence for episodic concentration and movement of carbonate sediments as a result of storm-wave action on a gently southward-sloping shelf [77]. In the current study, dolomite was produced by the digenesis of a carbonate ancestor, early aragonite, or most likely calcite. The dolomitization process of lime mud took place during early diagenesis, which probably led to the formation of the dolomite rhombs, which are fine crystalline and probably represent the first phase of dolomitization [78,79].

The mechanism of the shallowing upward in both gradual and non-gradual cycles has been mentioned by several authors [46–48,80–84]. The Milankovitch orbital forcing concept is the most crucial postulation (for allocyclic and autocyclic mechanisms). In this study, the analyses of the depositional cycles indicate a wide carbonate platform controlled by successive episodes of transgression resulting from differential subsidence, followed by a sea level fall because of the emergence of regressive episodes, which may be coupled with the MMCT. Thus, the origin of the shallowing-upward cycles is assigned to the fluctuations in the sea level caused by eustatic sea level fluctuations (an autocyclic mechanism) that form these cycles as well as their vertical repetition in a rhythmic way. Generally, the gradual emergence cycles indicate evenness between the rate of subsidence, the falling of sea level, and the rate of sedimentation [40]. These cycles point to the progressive change from one sub-environment to another, but without unexpected variation from deep to shallow facies [48]. It means that there is constant accommodation space during sedimentation. In the non-gradual cycle types 2, 4, and 6, the upper beds, which represent the shallower subtidal facies (grainstones and packstones), are absent as a result of increasing the rate of sea level falling without a sediment supply. The non-gradual cycle types 1, 3, and 5 are referred to due to the absence of the wackestone or lime mudstone textures that represent deep subtidal facies [48]. Such cycles occur when the sedimentation rate is lower than the transgression rate [40].

Therefore, the depositional history of the studied interval is based on three factors: the thickness variation, microfacies types, and the cyclicity of the microfacies. The thickness of the Marmarica Formation is relatively constant, assuming about less than 200 m in the Siwa Oasis and its surroundings. However, such thickness abruptly increases in the subsurface wells drilled in the narrow strip overlooking the Qattara wall. Additionally, in the Tarfa, Ghanem, Garf, Obeidalla, and Marzouk wells, the thickness of the Marmarica is 753 m, 714 m, 1070 m, 530 m, and 642 m, respectively [12]. Northwards along the narrow elongate strip (east-west), a very abrupt increase in thickness is encountered at the Kheima (639 m), Ganyen (900 m), Yidma (1113 m), and Washka (975 m) [12]. Between the above two basins, a narrow-uplifted strip has a thickness of less than 100 m. The possible explanation of the abrupt increase and decrease in the thickness of the Marmarica Formation suggests that there was continuous sedimentation of the Marmarica Formation in the down-faulted east-west basins separated by a structural high strip. Such a faulted zone may be affected by the structural control of the Nile Delta. Westwards, toward Salum and Libya, the thickness is nearly constant, which suggests a platform setting of the Marmarica Formation. This is contradicted by the opinion of [16,17], who postulated the ramp setting of the Marmarica Formation. Its nearly constant thickness toward the west may be due to a decrease in faulting structure away from the Nile Delta. The pelletal-peloidal packstone microfacies usually occur in the lower member of the Marmarica Formation. Microfacies that dominate the basal portion include lime mud and non-skeletal grains (intraclasts, pellets, and peloids). It may suggest deposition in a lagoonal setting with restricted and semi-restricted conditions [85]. Such an environment of deposition is quiet and has a high level of salinity [86,87]. Peloids are normally formed by the bio-erosion and destruction of microorganisms such as fungi and algae [88]. In lagoonal environments, micritization of the skeletal particles produces different types of peloids [89,90].

The presence of different types of fossils, such as echinoids, foraminifera, ostracods, and mollusks, in the wackestone and packstone microfacies points to a mesophotic to oligophotic, shallow open marine environment or on the proximal middle shelf (near and below the fair-water wave base) [91,92]. The richness of open marine fauna (echinoids, bryozoans, foraminifera, and molluscan debris) as well as the combination of micritic matrix indicate an open marine environment with low-medium energy and between the storm wave base and fair-weather wave base for deposition [35,93]. These microfacies were probably deposited in a deep marine environment with open water circulation, medium hydrodynamic energy, and normal salinity. The abundance of open marine skeletal fauna such as echinoderms, ostracods, benthonic foraminifera, and molluscan shell fragments, and the absence of reef-building fauna, are the evidence for this interpretation. The common wide distribution (vertical and lateral) of the above-mentioned skeletal particles in the study area suggests that they were deposited in an open marine platform setting. [17] mentioned that the Marmarica Formation includes two depositional sequences. A detailed field investigation of the Marmarica Formation shows no sequence boundary within this formation. However, this formation was built up in a cyclic sequence. All cycles are shallowing-upward (emergence type) and include gradual and non-gradual cyclic types [48]. The gradual cycles show the vertical arrangement of the microfacies. They begin with shale, followed by foraminiferal wackestone, and are capped by pelletal peloidal skeletal packstone (Figure 10). The cycle starts with claystone facies in a slightly deep subtidal environment, and then follows upward with foraminiferal wackestone microfacies, which indicate a shallow subtidal environment above the wave base. This cycle is capped by pelletal peloidal skeletal packstone, which forms the topmost part of the cycle, indicating a very shallow subtidal zone. The thickness of the lower shale increases eastward, pointing to the source of terrigenous clastic deposits. The characteristics of shales change in some cycles indicate deeper, low-energy; more restricted marine environments of the earliest deposition. It may also refer to marginal marine embayment with poor water circulation and temperature stratification. In deep subtidal areas, the water is usually cooler and does not permit the deposition of carbonate. The carbonate microfacies that commonly occur on the top of claystone in the middle and top of cycles show that the environment of deposition became shallower as well as less turbid, which led to the deposition of the upper carbonate microfacies in the gradual cycles. The gradual cycles manifested evenness between the rate of sedimentation and the sea level changes. Six non-gradual cycles were recognized in the Marmarica Formation at the studied sections (Figure 11). The non-gradual cycle may consist of one or two lithofacies or microfacies (wackestone or packstone) without claystone or lime-mudstone. It has the minimum thickness as compared with the gradual cycles. It is termed the condensed cycle [40] and the incomplete cycle [94]. It may indicate irregular changes in sea level. The non-gradual cycles describe the vertical arrangement of microfacies with some sub-environments missing, and they may indicate an irregular balance between the rate of sedimentation and subsidence [48].

7. Conclusions

The exposed Marmarica Formation outcrops at Gabal Western Bahi El-Din and Gabal El-Najdeen, Siwa Oasis, and the northern western Desert consist of fossiliferous limestone intercalated with dolomitic lime-mudstone, sandy limestone, and claystone. This formation is differentiated into three informal members: the lower, middle, and upper members. The lower member consists of limestones interbedded with sandy limestones, dolomitic limestone, calcarenite limestone, marley fossiliferous limestone, and thin beds of shale. The middle member is composed of yellowish-white limestone interbedded with sandy limestone, marley limestone, and shale. The upper member consists of white to yellowish white, massive, sandy, and chalky limestone. Chalky limestone is enriched with gastropods and pelecypods. The identified microfacies within this formation are skeletal lime-mudstone, dolomitic lime-mudstone, intraclastic wackestone, bryozoan wackestone, foraminiferal wackestone, foraminiferal bryozoan packstone, glauconitic molluscan packstone, molluscan intraclastic packstone, pelletal peloidal skeletal packstone, dolostones, and claystone microfacies. The vertical stacking pattern of microfacies led to the recognition of the emergence (shallowing-upward) type, which includes two types: gradual and non-gradual cycles. The gradual cycles denote the balance between the rate of subsidence, sea level oscillations, and the rate of sedimentation. The non-gradual cycles suggest variations in the sea level associated with structure. The depositional history of the Marmarica formation at this study interval relies on two factors: the types of microfacies and the cyclicity of the microfacies. The abundance of different skeletal particles (e.g., echinoids, foraminifera, ostracods, and mollusks) in the wackestone and packstone microfacies indicates mesophotic to oligophotic zones in shallow, open marine conditions.

Author Contributions: Conceptualization, M.A.K., A.S.Z., A.M.E.-H., E.Z. and A.M.K.; Data curation, M.A.K., A.S.Z., A.M.E.-H. and A.M.K.; Formal analysis, M.A.K., A.S.Z., A.M.E.-H. and A.M.K.; Funding acquisition, A.S.Z. and L.J.; Investigation, M.A.K., A.S.Z., A.M.E.-H. and A.M.K.; Methodology, M.A.K., A.S.Z., A.M.E.-H. and A.M.K.; Project administration, A.S.Z. and A.M.K.; Resources, A.S.Z., A.M.E.-H., E.Z. and A.M.K.; Software, A.S.Z., A.M.E.-H. and A.M.K.; Supervision, M.A.K., A.S.Z., E.Z. and A.M.K.; Validation, M.A.K., A.S.Z., A.M.E.-H. and A.M.K.; Visualization, A.S.Z., A.M.E.-H. and A.M.K.; Writing—original draft, M.A.K., A.S.Z., A.M.E.-H. and A.M.K.; Writing—review and editing, M.A.K., A.S.Z., L.J., A.M.E.-H., E.Z. and A.M.K. All authors have read and agreed to the published version of this manuscript.

Funding: L.J. and the CORE lab are supported by the Fundação de Amparo à Pesquisa do Estado de São Paulo (FAPESP) project 2016/24946-9. A.S.Z. is also supported by FAPESP grant number 2022/08285-3.

Data Availability Statement: Data supporting this paper are available upon request.

Acknowledgments: The authors express their gratitude to the two anonymous reviewers for devoting their time and effort to review this manuscript. We genuinely appreciate all of your insightful feedback, which enabled us to improve the manuscript.

Conflicts of Interest: The authors declare no conflict of interest.

References

1. Frigola, A.; Prange, M.; Schulz, M. Boundary Conditions for the Middle Miocene Climate Transition (MMCT v1.0). *Geosci. Model Dev.* **2018**, *11*, 1607–1626. [CrossRef]
2. Pound, M.J.; Haywood, A.M.; Salzmann, U.; Riding, J.B. Global Vegetation Dynamics and Latitudinal Temperature Gradients during the Mid to Late Miocene (15.97–5.33 Ma). *Earth-Sci. Rev.* **2012**, *112*, 1–22. [CrossRef]
3. Billups, K.; Schrag, D.P. Paleotemperatures and Ice Volume of the Past 27 Myr Revisited with Paired Mg/Ca and $^{18}O/^{16}O$ Measurements on Benthic Foraminifera. *Paleoceanography* **2002**, *17*, 3-1–3-11. [CrossRef]
4. Shevenell, A.E.; Kennett, J.P.; Lea, D.W. Middle Miocene Ice Sheet Dynamics, Deep-Sea Temperatures, and Carbon Cycling: A Southern Ocean Perspective. *Geochem. Geophys. Geosystems* **2008**, *9*, Q02006. [CrossRef]
5. Lear, C.H.; Mawbey, E.M.; Rosenthal, Y. Cenozoic Benthic Foraminiferal Mg/Ca and Li/Ca Records: Toward Unlocking Temperatures and Saturation States: Ocean temperatures and saturation state. *Paleoceanography* **2010**, *25*, PA4215. [CrossRef]
6. Haq, B.U.; Hardenbol, J.; Vail, P.R. Chronology of Fluctuating Sea Levels Since the Triassic. *Science* **1987**, *235*, 1156–1167. [CrossRef] [PubMed]
7. Kominz, M.A.; Browning, J.V.; Miller, K.G.; Sugarman, P.J.; Mizintseva, S.; Scotese, C.R. Late Cretaceous to Miocene Sea-level Estimates from the New Jersey and Delaware Coastal Plain Coreholes: An Error Analysis. *Basin Res.* **2008**, *20*, 211–226. [CrossRef]
8. John, C.M.; Karner, G.D.; Browning, E.; Leckie, R.M.; Mateo, Z.; Carson, B.; Lowery, C. Timing and Magnitude of Miocene Eustasy Derived from the Mixed Siliciclastic-Carbonate Stratigraphic Record of the Northeastern Australian Margin. *Earth Planet. Sci. Lett.* **2011**, *304*, 455–467. [CrossRef]
9. Buchbinder, B. *Miocene Carbonates of the Eastern Mediterranean, the Red Sea and the Mesopotamian Basin: Geodynamic and Eustatic Controls*; The Society for Sedimentary Geology: Tulsa, OK, USA, 1996.
10. Piller, W.E.; Harzhauser, M.; Mandic, O. Miocene Central Paratethys Stratigraphy–Current Status and Future Directions. *Stratigraphy* **2007**, *4*, 151–168. [CrossRef]
11. Mutti, M.; Piller, W.; Betzler, C. (Eds.) *Miocene Carbonate Systems: An Introduction. Oligocene–Miocene Carbonate Systems*, 1st ed.; The International Accreditation Service: Geneva, Switzerland, 2010; Volume 42.
12. Said, R. *The Geology of Egypt: Balkema*; Brookfield: Rotterdam, The Netherlands, 1990; Volume 734.
13. Abdulsamad, E.O.; Bu-Argoub, F.M.; Tmalla, A.F.A. A Stratigraphic Review of the Eocene to Miocene Rock Units in the al Jabal al Akhdar, NE Libya. *Mar. Pet. Geol.* **2009**, *26*, 1228–1239. [CrossRef]
14. Gindy, A.R.; El Askary, M.A. Stratigraphy, Structure, and Origin of Siwa Depression, Western Desert of Egypt. *AAPG Bull.* **1969**, *53*, 603–625.
15. Tamish, M.O.; Holail, H.M.; El-Askary, M.A.; Sadek, A. Lithostratigraphy, Facies Analysis and Depositional Environments of the Middle Miocene Carbonate Rocks, Northwestern Desert, Egypt. *Bull. Fac. Sci. Alex. Univ.* **1996**, *1*, 251–264.
16. Abdel-Fattah, Z.A.; Kora, M.A.; Ayyad, S.N. Facies Architecture and Depositional Development of Middle Miocene Carbonate Strata at Siwa Oasis, Northwestern Egypt. *Facies* **2013**, *59*, 505–528. [CrossRef]
17. Anan, T.; Reda, A.; El Belasy, A.; El-Shahat, A. Facies Analysis and Sequence Stratigraphy of the Middle Miocene Marmarica Formation at Siwa Area, North Western Desert, Egypt. *Geol. J.* **2022**, *57*, 2749–2769. [CrossRef]

18. Gindi, A.; Abd-Alla, M.A. Stable Isotopes and Microfacies of the Middle Miocene Marmarica Formation, North Western Desert, Egypt. *Egypt. J. Geol* **2000**, *44*, 109–125.
19. Farouk, S.; Khalifa, M.A. Facies Tracts and Sequence Development of the Middle Eocene–Middle Miocene Successions of the Southwestern Qattara Depression, Northern Western Desert, Egypt. *Palaontol. Stratigr. Fazies* **2010**, *18*, 195–215.
20. Said, R. *The Geology of Egypt*; Elsevier: Amsterdam, The Netherlands, 1962; Volume 377.
21. Hantar, G. North Western Desert. In *The Geology of Egypt*; Balkema, A.A., Ed.; Brookfield: Rotterdam, The Netherlands, 1990; pp. 293–319.
22. Issawi, B.; Francis, M.H.; Youssef, E.A.A.; Osman, R.A. *The Phanerozoic Geology of Egypt: A Geodynamic Approach: Special Publication, 81*; Ministry of Petroleum: Cairo, Egypt, 2009.
23. Marzouk, I. Rock Stratigraphy and Oil Potentialities of the Oligocene and Miocene in the Western Desert of Egypt. In Proceedings of the 7th Arab Petroleum Congress, Kuwait, 16–22 March 1970; Volume 54, pp. 1–37.
24. Schlumberger Middle East. *Geology of Egypt*; Schlumberger Middle East: Cairo, Egypt, 1984; pp. 1–64.
25. Ouda, K. Biostratigraphy, Paleoecology and Paleogeography of the Middle and Late Tertiary Deposits of the Northern Western Desert, Egypt. *NEUES Jahrb. Geol. PALAONTOLOGIE Abh.* **1998**, *207*, 311–394. [CrossRef]
26. Dunham, R.J. Classification of Carbonate Rocks According to Depositional Textures. In *Classification of Carbonate Rocks—A Symposium*; AAPG: Tulsa, OK, USA, 1962; Volume 38, pp. 108–121.
27. Embry, A.F.; Klovan, J.E. A Late Devonian Reef Tract on Northeastern Banks Island, NWT. *Bull. Can. Pet. Geol.* **1971**, *19*, 730–781.
28. Coward, M.P.; Ries, A.C. Tectonic Development of North African Basins. *Geol. Soc. Lond. Spec. Publ.* **2003**, *207*, 61–83. [CrossRef]
29. Guiraud, R.; Bosworth, W.; Thierry, J.; Delplanque, A. Phanerozoic Geological Evolution of Northern and Central Africa: An Overview. *J. Afr. Earth Sci.* **2005**, *43*, 83–143. [CrossRef]
30. Rosendahl, B.R.; Kilembe, E.; Kaczmarick, K. Comparison of the Tanganyika, Malawi, Rukwa and Turkana Rift Zones from Analyses of Seismic Reflection Data. *Tectonophysics* **1992**, *213*, 235–256. [CrossRef]
31. Holail, H.; Tamish, M.; El-Askary, M.; Sadek, A. Geochemistry and Diagenesis of Middle Miocene Carbonate Rocks, Northern Western Desert, Egypt. *Neues Jahrb. Geol. Paläontol.-Monatsh.* **1997**, 191–212. [CrossRef]
32. El-Shazly, S.H.; Abdel-Hamid, M. Contribution to the Middle Miocene Megafossils from Siwa Oasis, Western Desert, Egypt. *Egypt. J. Paleontol.* **2001**, *1*, 263–297.
33. El-Sabbagh, A.M.; El Hedeny, M.M. A Shell Concentration of the Middle Miocene Crassostrea Gryphoides (Schlotheim, 1813) from Siwa Oasis, Western Desert, Egypt. *J. Afr. Earth Sci.* **2016**, *120*, 1–11. [CrossRef]
34. El-Sabbagh, A.; El-Hedeny, M.; Al Farraj, S. Thalassinoides in the Middle Miocene Succession at Siwa Oasis, Northwestern Egypt. *Proc. Geol. Assoc.* **2017**, *128*, 222–233. [CrossRef]
35. Flügel, E. *Microfacies of Carbonate Rocks: Analysis, Interpretation and Application*; Springer: Berlin/Heidelberg, Germany; New York, NY, USA, 2004; p. 976.
36. Gregg, J.M.; Sibley, D.F. Epigenetic Dolomitization and the Origin of Xenotopic Dolomite Texture. *J. Sediment. Res.* **1984**, *54*, 908–931.
37. Gregg, J.M. Origins of Dolomite in the Offshore Facies of the Bonneterre Formation (Cambrian), Southeast Missouri. In *Sedimentology and Geochemistry of Dolostones*; Shukla, V., Baker, P.A., Eds.; The Society for Sedimentary Geology: Tulsa, OK, USA, 1988; Volume 43, ISBN 978-1-56576-169-8.
38. Wright, W.R. Dolomitization, Fluid-Flow and Mineralization of the Lower Carboniferous Rocks of the Irish Midlands and Dublin Basin Regions. Ph.D. Thesis, University College Dublin, Dublin, Ireland, 2001.
39. Fisher, A.G. The Lofer Cyclothems of the Alpine Triassic. *Bull. Kans. Geol. Surv.* **1964**, *169*, 107–149.
40. Grotzinger, J.P. Cyclicity and Paleoenvironmental Dynamics, Rocknest Platform, Northwest Canada. *Geol. Soc. Am. Bull.* **1986**, *97*, 1208–1231. [CrossRef]
41. Goldhammer, R.K.; Dunn, P.A.; Hardie, L.A. High Frequency Glacio-Eustatic Sealevel Oscillations with Milankovitch Characteristics Recorded in Middle Triassic Platform Carbonates in Northern Italy. *Am. J. Sci.* **1987**, *287*, 853–892. [CrossRef]
42. Goldhammer, R.K.; Dunn, P.A.; Hardie, L.A. Depositional Cycles, Composite Sea-Level Changes, Cycle Stacking Patterns, and the Hierarchy of Stratigraphic Forcing: Examples from Alpine Triassic Platform Carbonates. *Geol. Soc. Am. Bull.* **1990**, *102*, 535–562. [CrossRef]
43. Strasser, A. Shallowing-upward Sequences in Purbeckian Peritidal Carbonates (Lowermost Cretaceous, Swiss and French Jura Mountains). *Sedimentology* **1988**, *35*, 369–383. [CrossRef]
44. Haas, J. A Basic Model for Lofer Cycles. In *Cycles and Events in Stratigraphy*; Springer: Berlin/Heidelberg, Germany, 1991; pp. 722–732.
45. Osleger, D. Subtidal Carbonate Cycles: Implications for Allocyclic vs. Autocyclic Controls. *Geology* **1991**, *19*, 917–920. [CrossRef]
46. Satterley, A.K. Cyclic Carbonate Sedimentation in the Upper Triassic Dachstein Limestone, Austria; the Role of Patterns of Sediment Supply and Tectonics in a Platform-Reef-Basin System. *J. Sediment. Res.* **1996**, *66*, 307–323.
47. Satterley, A.K. The Interpretation of Cyclic Successions of the Middle and Upper Triassic of the Northern and Southern Alps. *Earth-Sci. Rev.* **1996**, *40*, 181–207. [CrossRef]
48. Khalifa, M.A. Depositional Cycles in Relation to Sea Level Changes, Case Studies from Egypt and Saudi Arabia. *Egypt. J. Geol.* **1996**, *40*, 141–171.
49. Enos, P.; Samankassou, E. Lofer Cyclothems Revisited (Late Triassic, Northern Alps, Austria). *Facies* **1998**, *38*, 207–227. [CrossRef]

50. Haas, J.; Lobitzer, H.; Monostori, M. Characteristics of the Lofer Cyclicity in the Type Locality of the Dachstein Limestone (Dachstein Plateau, Austria). *Facies* **2007**, *53*, 113–126. [CrossRef]
51. Gindy, A.R. The Relative Diagenetic Order of Preservation of Skeletal Structures in Fossil Debris of a Miocene Coquina near Salûm, Egypt. *Neues Jahrb. Geol. Paläontol. Monatsh.* **1987**, *1*, 27–42. [CrossRef]
52. El-Shahat, A. Middle Miocene Carbonates from the Northern Plateau of the Western Desert (Egypt): Petrography and Geochemistry. *Facies* **1993**, *28*, 67–76. [CrossRef]
53. Gameil, M.; Sadek, S. Stratigraphy, Megafossil Content and Microfacies Analysis of the Middle Miocene Rocks, East Matruh, Northwestern Egypt. 2nd Inter Conf Geo-Resources in the Middle East and North Africa (Germena). *Cairo Univ.* **2007**, *2*, 3–28.
54. Khalifa, M.; Al-Kahtany, K.; Farouk, S.; El-Sorogy, A.S.; Al Qahtani, A. Microfacies Architecture and Depositional History of the Upper Jurassic (Kimmeridgian) Jubaila Formation in Central Saudi Arabia. *J. Afr. Earth Sci.* **2021**, *174*, 104076. [CrossRef]
55. Ali, C.A.; Mohamed, K.R. Microfacies and Diagenesis in the Setul Limestone in Langkawi and Perlis. *Bull. Geol. Soc. Malays.* **2013**, *59*, 59–66. [CrossRef]
56. Wilson, J.L. The Lower Carboniferous Waulsortian Facies. In *Carbonate Facies in Geologic History*; Springer: New York, NY, USA, 1975; pp. 148–168, ISBN 978-0-387-90343-9.
57. Lee, Y.I.; Kim, J.C. Storm-influenced Siliciclastic and Carbonate Ramp Deposits, the Lower Ordovician Dumugol Formation, South Korea. *Sedimentology* **1992**, *39*, 951–969. [CrossRef]
58. Hiscott, R.N. Tidal Deposits of the Lower Cambrian Random Formation, Eastern Newfoundland: Facies and Paleoenvironments. *Can. J. Earth Sci.* **1982**, *19*, 2028–2042. [CrossRef]
59. Smith, S.A.; Hiscott, R.N. Latest Precambrian to Early Cambrian Basin Evolution, Fortune Bay, Newfoundland: Fault-Bounded Basin to Platform. *Can. J. Earth Sci.* **1984**, *21*, 1379–1392. [CrossRef]
60. Odin, G.S.; Fullagar, P.D. Chapter C4 Geological Significance of the Glaucony Facies. In *Developments in Sedimentology*; Elsevier: Amsterdam, The Netherlands, 1988; Volume 45, pp. 295–332.
61. Hesse, R. Silica Diagenesis: Origin of Inorganic and Replacement Cherts. *Earth-Sci. Rev.* **1989**, *26*, 253–284. [CrossRef]
62. Thambunya, S.; Pisutha-Arnond, V.; Khantaprab, C. Depositional Environments of Permian Rocks of the Khao Khad Formation in Central Thailand. *ScienceAsia* **2007**, *33*, 371–381. [CrossRef]
63. Longman, M.W. Carbonate Diagenetic Textures from Nearsurface Diagenetic Environments. *AAPG Bull.* **1980**, *64*, 461–487.
64. Whalen, M.T. Depositional History of an Upper Triassic Drowned Carbonate Platform Sequence: Wallowa Terrane, Oregon and Idaho. *Geol. Soc. Am. Bull.* **1988**, *100*, 1097–1110. [CrossRef]
65. Ziko, A.; El-Sorogy, A.S.; Zalat, A.; Eweda, S.; Saber, N. Middle Miocene Bryozoa from Siwa Oasis, Western Desert, Egypt. In Proceedings of the 5th International Conference of Geology of the Arab World: Cairo University, Cairo, Egypt, 21–24 February 2000; pp. 1465–1496.
66. Hallock, P.; Glenn, E.C. Larger Foraminifera: A Tool for Paleoenvironmental Analysis of Cenozoic Carbonate Depositional Facies. *Palaios* **1986**, *1*, 55–64. [CrossRef]
67. Kumar, P.; Saraswati, P.K.; Banerjee, S. Early Miocene Shell Concentration in the Mixed Carbonate-Siliciclastic System of Kutch and Their Distribution in Sequence Stratigraphic Framework. *J. Geol. Soc. India* **2009**, *74*, 432–444. [CrossRef]
68. Heckel, P.H. Recognition of Ancient Shallow Marine Environments. In *Recognition of Ancient Sedimentary Environments*; Rigby, J.K., Hamblin, W.K., Eds.; The Society for Sedimentary Geology: Tulsa, OK, USA, 1972; Volume 16, pp. 226–286, ISBN 978-1-56576-146-9.
69. Kulm, L.D.; Roush, R.C.; Harlett, J.C.; Neudeck, R.H.; Chambers, D.M.; Runge, E.J. Oregon Continental Shelf Sedimentation: Interrelationships of Facies Distribution and Sedimentary Processes. *J. Geol.* **1975**, *83*, 145–175. [CrossRef]
70. Ziegler, B. Ammoniten-Ökologie am Beispiel des Oberjura. *Geol. Rundsch.* **1967**, *56*, 439–464. [CrossRef]
71. Harris, M.K.; Thayer, P.A.; Amidon, M.B. Sedimentology and Depositional Environments of Middle Eocene Terrigenous-Carbonate Strata, Southeastern Atlantic Coastal Plain, USA. *Sediment. Geol.* **1997**, *108*, 141–161. [CrossRef]
72. Amorosi, A. Detecting Compositional, Spatial, and Temporal Attributes of Glaucony: A Tool for Provenance Research. *Sediment. Geol.* **1997**, *109*, 135–153. [CrossRef]
73. McRae, S.G. Glauconite. *Earth-Sci. Rev.* **1972**, *8*, 397–440. [CrossRef]
74. Huggett, J.M. Scanning Electron Microscope and X-ray Diffraction Investigations of Mudrock Fabrics, Textures and Mineralogy. *Scan. Microsc.* **1989**, *3*, 12.
75. Snedden, J.W.; Kersey, D.G. Origin of San Miguel Lignite Deposit and Associated Lithofacies, Jackson Group, South Texas. *AAPG Bull.* **1981**, *65*, 1099–1109.
76. Haldar, S.K. *Introduction to Mineralogy and Petrology*; Elsevier: Amsterdam, The Netherlands, 2020.
77. Brett, C.E. Sedimentology, Facies and Depositional Environments of the Rochester Shale (Silurian; Wenlockian) in Western New York and Ontario. *J. Sediment. Petrol.* **1983**, *53*, 947–971.
78. Morrow, D.W. Diagenesis 1. Dolomite-Part 1: The Chemistry of Dolomitization and Dolomite Precipitation. *Geosci. Can.* **1982**, *9*, 5–13.
79. Al-Aasm, I.S.; Packard, J.J. Stabilization of Early-Formed Dolomite: A Tale of Divergence from Two Mississippian Dolomites. *Sediment. Geol.* **2000**, *131*, 97–108. [CrossRef]
80. Ginsburg, R.N. Landward Movement of Carbonate Mud: New Model for Regressive Cycles in Carbonates. *AAPG Bull.* **1971**, *55*, 340.
81. James, N.P. Shallowing-Upward Sequences in Carbon-Ates. *Facies Models* **1984**, *1*, 213–228.
82. Hardie, L.A. Carbonate Depositional. Environments, Modern and Ancient: Part 3: Tidal Fiats. *Colo. Sch. Mines Q.* **1986**, *81*, 1–74.

83. Koerschner, W.F.; Read, J.F. Field and Modelling Studies of Cambrian Carbonate Cycles, Virginia, Appalachians. *J. Sediment. Res.* **1989**, *59*, 654–687. [CrossRef]
84. Elrick, M.; Read, J.F. Cyclic Ramp-to-Basin Carbonate Deposits, Lower Mississippian, Wyoming and Montana; a Combined Field and Computer Modeling Study. *J. Sediment. Petrol.* **1991**, *61*, 1194–1224.
85. Brandano, M.; Frezza, V.; Tomassetti, L.; Pedley, M.; Matteucci, R. Facies Analysis and Palaeoenvironmental Interpretation of the Late Oligocene Attard Member (Lower Coralline Limestone Formation), Malta. *Sedimentology* **2009**, *56*, 1138–1158. [CrossRef]
86. Read, J.F. Carbonate Platform Facies Models. *AAPG Bull.* **1985**, *69*, 1–21.
87. Tucker, M.A. *Sedimentary Petrology*, 3rd ed.; Blackwell Publishing: Oxford, UK, 2008.
88. Adachi, N.; Ezaki, Y.; Liu, J. The Fabrics and Origins of Peloids Immediately after the End-Permian Extinction, Guizhou Province, South China. *Sediment. Geol.* **2004**, *164*, 161–178. [CrossRef]
89. Tucker, M.E.; Wright, V.P. *Carbonate Sedimentology*; Blackwell Scientific Publication: Hoboken, NJ, USA, 1990.
90. Flügel, E. *Microfacies of Carbonate Rocks: Analysis, Interpretation and Application*, 2nd ed.; Springer: Berlin/Heidelberg, Germany, 2010; ISBN 978-3-642-03795-5.
91. Geel, T. Recognition of Stratigraphic Sequences in Carbonate Platform and Slope Deposits: Empirical Models Based on Microfacies Analysis of Palaeogene Deposits in Southeastern Spain. *Palaeogeogr. Palaeoclimatol. Palaeoecol.* **2000**, *155*, 211–238. [CrossRef]
92. Pomar, L.; Brandano, M.; Westphal, H. Environmental Factors Influencing Skeletal Grain Sediment Associations: A Critical Review of Miocene Examples from the Western Mediterranean. *Sedimentology* **2004**, *51*, 627–651. [CrossRef]
93. Pomar, L. Types of Carbonate Platforms: A Genetic Approach. *Basin Res.* **2001**, *13*, 313–334. [CrossRef]
94. Khalifa, M.A. Lithofacies, Diagenesis and Cyclicity of the 'Lower Member' of the Khuff Formation (Late Permian), Al Qasim Province, Saudi Arabia. *J. Asian Earth Sci.* **2005**, *25*, 719–734. [CrossRef]